UNIVERSITY OF ZIMBABWE

FACULTY OF ENGINEERING

DEPARTMENT OF CIVIL ENGINEERING

Remote sensing based estimation of evaporation among different land cover types in the Mkindo catchment, Upper Wami basin-Tanzania

ASHA MOHAMED

MSc Thesis in IWRM

Harare, June 2010

in collaboration with

Remote sensing based estimation of evaporation among different land cover types in the Upper-Wami River Basin, Tanzania

Master of Science Thesis

by

Asha Mohamed

Supervisors

Dr. Amon Murwira

Dr. Victor Kongo

Mr. Eugene Makaya

A thesis submitted in partial fulfillment of the requirements for the degree of Master of Science in Integrated Water Resources Management of the University of Zimbabwe

Harare

June 2010

DECLARATION

I, ASHA MOHAMED declare that this is my own work, a result of my own investigation. All the sources that I have used or quoted have been indicated and acknowledged by means of complete references. To the best of my knowledge, this work has not been submitted before for degree award at any other university.

Signed: …………………………………

Date: …………………………………….

The findings, interpretations and conclusions expressed in this study do neither reflect the views of the University of Zimbabwe, Department of Civil Engineering nor of the individual members of the MSc Examination Committee, nor of their respective employers.

DEDICATION

I am dedicating this work to my beloved mother Lailat B. Mhamilawa, may God YAHWE favor and bless you abundantly.

ABSTRACT

In Semi-arid Africa, evaporation is the dominant hydrological flux and hence an important component in water resources management. However, it is a challenge to fairly estimate the spatial variation of evaporation especially on composite terrains due to heterogeneity of the landscape. This is further compounded by the uncertainties associated with the various approaches used for estimating the flux, most of which are based on extrapolating point observations. In the recent past, there has been progress in developing and validating various remote sensing algorithms for computing evaporation over large spatial extents.

One such algorithm, the Surface Energy Balance System (SEBS) was applied in the Mkindo catchment, located in the upper-Wami River basin in Tanzania using the Moderate Resolution Imaging Spectroradiometer (MODIS) satellite images. Six images covering June 2008 to September 2009 were analyzed together with a land use map of the same area. The SEBS evaporation estimates were compared with the potential evaporation over the Mkindo catchment.

SEBS results showed good correlation with the computed Potential evaporation computed from climatological parameter in the catchment, with different land uses/cover types having different evaporative water use signature, on both daily and monthly time scale. Forest and irrigated agriculture land use, located on the lower parts of the catchment, had relatively higher evaporative water use compared to the other land uses in the catchment.

Key words:

Evaporation, land use, SEBS Wami basin, water use

AKNOWLEDGEMENT

In completion of this thesis, I am indebted to many without whose help and expertise it would have been difficult to carry out.

To my LORD Jesus Christ the only true hope.

My most sincere thanks go to my supervisors, Doctor Amon Murwira and Victor Kongo, for guiding me throughout the course of this thesis and to Mr. Eugene Makaya. Thanks to Lichun Wang from ITC for technical support on the use of SEBS and its related softwares.

Thanks to Sokoine University of Agriculture especially professor Mahoo and Wami River Basin staffs, particularly, Florence Mahay, for a close support whenever it was needed and data provision. I am also, very grateful to the Stockholm Environment Institute (SEI) Africa center, for accommodating and facilitating me for 4 months during my field work in the Wami river basin. Special thanks to Jacqueline Senyagwa, your kindness will be rewarded before the LORD.

To Lucas Kwezi, you have inspired me so much, encouraged, and helped me in ways words can’t explain; you perfectly played your part.

I also, owe much gratitude to my family and more earnestly to my mother; you are a woman and a half, to Mniga, my young boy Goodluck, and all others who supported me in my Endeavour’s.

To my IWRM classmates thank you for encouragement.

LIST OF ACRONYMS

SEBS	Surface Energy Balance System
NDVI	Normalized Difference Vegetation Index
MODIS	Moderate Resolution Imaging Spectroradiometer
GIS	Geographic Information System
GPS	Global Positioning System
RS	Remote Sensing
NASA	the National Aeronautics and Space Administration

TABLE OF CONTENTS

LIST OF TABLES

LIST OF FIGURES

1.0 INTRODUCTION

Water resources management at a basin scale is a widely accepted idea and strategies for better management have to be done at this scale for improved effective local participation (Kidd and Quinn, 2005). In Southern Africa water resources management policies and strategies are formulated at the scale of a basin (Jaspers, 2001; Jaspers 2003; Manzungu, 2004; Tapela, 2006). However, the hydrological processes inside a basin are not straight forward as it may look, due to reasons like the natural processes as well as man made structures like dams or diversion canals which tend to interfere and influence hydrological processes. This makes it necessary to understand how hydrological processes operate at the basin scale.

Evaporation (total) is the second largest component of water balance in semi arid basins (Kongo, 2008). It is also claimed that, evaporation is the prime process of water transfer in the hydrological cycle (Lin, 2006) and it plays a major role in linking water balance and surface energy balance, making it an important component in water planning.

However, of all the components of the hydrological cycle, evaporation is one the most difficult to estimate owing to complex interactions between the components of the land-plant-atmosphere system (Hughes, 2001).Also, due to the complex nature of mixed vegetation and different land use patterns in a basin, estimating evaporation using point measurement (Hemakumara et al., 2003) has high chances of not giving valid estimates especially in Southern Africa where the hydrological measurement network is poorly distributed (Mul, 2009) and very few monitoring networks are in place. However, evaporation estimates are needed in a wide array of problems in hydrology, agronomy, forestry and land resources planning, such as water balance computation, irrigation management, river flow forecasting, investigation of lake chemistry and ecosystem modeling, (Avissar and Pielke, 1989; Anderson et al., 2003; Moran, 2004).

1.1 Description of the problem

Review of literature highlight the challenges associated with estimating evaporation especially on composite terrains due to heterogeneity of the landscape and differences in land cover types (Hemakumara et al., 2003). The approaches of estimating evaporation in place are based on extrapolation of point based observations (Kongo, 2008) which tend to overlook the fact that evaporation is a continuous variable and different land use/cover types have different evaporation signature. For example using Epan to measure evaporation in a mixed vegetation portion of land will not give representative results.

1.2 Justification of the study

Now, rapidly increasing population, improved living standards as well as climate change is posing great pressure on fresh water resources which is only 3% of the world waters (Gumbo, et al., 2001) and (Cong et al., 2009). Global warming is expected to increase evaporation, meaning the fresh water resources on the globe will be lessened further.

In the Mkindo catchment, evaporation is a dominant hydrological flux. In addition to that, the catchment is characterized by different landscapes and land cover types which calls for a great urge for a better and accurate knowledge and proper quantification of evaporation. This research focused on the satellite derived total evaporation in order to characterize the spatial and temporal variability of evaporation in Mkindo sub-catchment. The results are of importance to water balance studies and water resources management in general and hence sustainable water management in the Mkindo catchment.

1.3 Research Objectives

1.3.1 Main Objective

The main objective of this research work was to determine the influence of land uses on evaporation using Moderate-resolution Imaging Spectroradiometer (MODIS) satellite based Surface Energy Balance System (SEBS) in the Mkindo sub catchment of Upper Wami Basin, Tanzania.

1.3.2 Specific Objectives

1. To determine the spatial distribution of total evaporation in the Mkindo sub catchment in 2008/2009 by season using Surface Energy Balance System
2. To test whether evaporation significantly varies by land cover type
3. To establish the contribution of the respective land cover to total evaporation in the Mkindo sub catchment in 2008/2009 by season
4. To compare the total evaporation values of the SEBS modeled evaporation and calculated evapotranspiration.

1.4 Research Questions

On completion of this research work the following questions will be answered:

- Is evaporation distribution patterns space and time dependent in the Mkindo catchment?
- Does the spatial land cover/use distribution pattern influence evaporation spatiality?
- Are the SEBS evaporation results in line with calculated results?

1.5 Outline of the Thesis

This thesis consists of five chapters.

Chapter two consists of Literature review on land cover, estimation of evaporation and Surface Energy Balance System method of estimating evaporation.

Chapter three comprises of the description of the study area and the detailed explanation of the methods used in the research.

Chapter four explains the results, discussion and limitations of the study; and

Chapter five concludes and gives recommendations.

2.0 STATE OF KNOWLEDGE ON ESTIMATION OF EVAPORATION: A REVIEW

Evaporation requires a large amount of energy to occur. This makes possible prediction of actual evaporation using the energy balance principle (Su, 2002). The values of components in the energy balance equation can be determined with remote sensors and for this reason the use of remote sensing technology in estimation of Actual ET.

Also, Satellite remote sensing is potentially a useful tool for landscape scale hydrologic analysis because of the global continuity of the observations (Bastiaanssen et al., 1998). It is therefore the technique which provides representative measurements of several relevant physical parameters at point scale to the whole globe.

This research will use remote sensing and GIS tools to estimate total evaporation, together with advanced technology for gathering data and processing.

On the other hand, land cover/use (vegetation cover) is strongly related to climatic conditions because it governs the partitioning of heat balance terms and influencing soil moisture. In this way land cover/use alters the long term balance of the hydrological cycle. Therefore, land cover has immediate and long lasting impacts on the terrestrial hydrology (Calder, 1993). This is because different land covers influence general circulation models directly through the parameters of the atmospheric model or indirectly through the hydrologic coupling.

2.1 Land Cover

Barnsley (2001) gave an explanation of land cover as physical material on the surface of a given parcel of land (example grass, concrete, tarmac, and water). Land cover can also be explained as the upper cover of the earth's surface, for example, vegetation, built up area or urban, infrastructure, water, barren land as well as features like mountains and others. Concepts concerning land cover and land use activity are closely related and in many cases have been used interchangeably. The purposes for which lands are being used commonly have associated types of cover, whether forest, agricultural, residential, or industrial.

Land cover is an essential variable for human beings livelihood and for this reason; it is mostly anthropogenic activities that affects land cover than natural processes. High population growth and over dependency on the environment are the major contributors of fast growing detrimental land covers in Africa South of Sahara desert (Tekele and Hedlund, 2000).

Remote sensing image-forming devices do not record activity directly. The remote sensor acquires a response which is based on many characteristics of the land surface, including natural or artificial cover. The interpreter uses patterns, tones, textures, shapes, and site associations to derive information about land use activities from what is basically information about land cover.

2.2 Land Cover Classification

Land cover classification as an idea was developed as long back as early 1970's (Anderson, 1976). Since then a large number of land cover classification exists, ranging from supervised to unsupervised. Supervised classification uses similarity of cases to a set of predefined classes that have been characterized spectrally while unsupervised classification groups cases by their relative spectral similarity. The best land cover data when compared to others, remotely sensed imagery are very useful in obtaining spatial and temporal details about land cover.

2.3 Land Cover Change and its influence on the Hydrological Cycle

Land-cover change in this context means change in surface greenness or change in vegetation pattern. Studies show that, global vegetation cover strongly relates to climatic conditions. Land-cover influences the hydrological cycle through governing the partitioning of the heat balance term and influencing soil moisture characteristics and thus in most of the cases, land cover changes has been accompanied with high flows and change in seasonal stream flows as well as evaporation increase (Kebede, 2009).

Moreover, number of studies has been conducted in Africa on the impacts of land cover on water resources like that of. Andrews and Bullock (1994) in East and Southern Africa on effects of afforestation and deforestation on runoff, (Lorup et al., 1998) explaining the effects of land use and land cover on runoff in Africa. In Tanzania, Kashaigili, (2008) carried a study on the effects of land use and land cover change on runoff or flow regime. These studies express that different land cover types have different influence in the hydrological cycle. However, in most studies land cover/use change is mainly linked to hydrological cycle alteration though specifically to processes such as infiltration, ground water recharge, and run off ignoring the effect of land cover and change on evaporation while in fact land cover/use has very significant influence on evapotranspiration.

2.4 Land Surface Evaporation

Evaporation is the water that has been transformed from surface waters which are in liquid state to water in gaseous state or vapor and transported to the atmosphere (Brutsaert, W., 2005). Evapotranspiration (ET) refers to the conversion of water into water vapour by the dual process of evaporation from the soil and transpiration (the escape of water though plant's stomata).

Total evaporation comprises of open water evaporation, evapotranspiration and interception (Tsiko et al, 2010). Evaporation tend to vary with regions and seasons (Kwast et al., 2009) and due to this variation nature water managers whose main tasks are planning and adjudicating the distribution of water resources need to have clear understanding of the evaporation process and its spatial and temporal variation. This information gives support to precision irrigation, determining crop water stress and water use of vulnerable ecosystems. Also, it is very helpful in predicting weather and climate change.

2.4.1 Role of evaporation in Hydrologic Modelling

Evaporation and precipitation are the most important components of most of hydrologic models (Beven, 1993, De Groen, 2002, Beven, 2004). In modelling catchment water balance the prime output is total evaporation making evaporation a very important component.

2.5 Estimation of Evaporation

Attempts to come up with accurate measurements of evaporation have been taking place continuously. There are number of methods for estimating evaporation which have been developed, these methods can measure evaporation on water bodies, land surface and from plants. The methods for determining evaporation can be grouped into several categories, including;

2.5.1 Water Balance Approach

This approach involves the estimation of evaporation by the use of water balance equation. It considers evaporation as residual after deducting other uses from total precipitation. The water budget methods are simple in theory, but rarely produce reliable results in practice. The main difficulty is that some of the variables, such as seepage rate in a water system, are hard to measure (Singh, 1989). Morton (1990) has summarized other problems associated, in general, with such methods. The water balance equation states:

$$\mathbf{E = P - Q - G_{out} - \Delta S}$$

(Eq. 1)

where,

E = Total evaporation, **P** = Precipitation, **Q** = Run off, $\mathbf{G_{out}}$ **=** Ground water out flow and **ΔS** = Change in storage

Lysimeter method is the technique widely used in the water balance approach method, where an artificial soil volume is used to determine the actual evaporation. This method is used in natural environment by accurately measuring other components of the water balance.

2.5.2 Hydrological Models Approach

Hydrologic models are simplified, conceptual representations of a part of the hydrologic cycle. They are used for hydrologic prediction and for understanding hydrologic processes. The main objective of hydrological modeling is to explain the variability of catchment response in terms of the factors that may influence it (Beven, 2004). Hydrological models normally work by simulation, where by all the intermediate processes such as evaporation, interception, infiltration, ground water and transpiration are taken into account.

$$ET_o = \frac{0.408\Delta(R_n - G) + \gamma \frac{900}{T+273} u_2 (e_s - e_a)}{\Delta + \gamma(1 + 0.34 u_2)} \quad \text{(Eq. 2)}$$

where

ET_o reference evapotranspiration [mm day^{-1}],
R_n net radiation at the crop surface [MJ m^{-2} day^{-1}],
G soil heat flux density [MJ m^{-2} day^{-1}],
T mean daily air temperature at 2 m height [°C],
u_2 wind speed at 2 m height [m s^{-1}],
e_s saturation vapor pressure [kPa],
e_a actual vapor pressure [kPa],
e_s - e_a saturation vapor pressure deficit [kPa],
D slope vapor pressure curve [kPa $°C^{-1}$],
g psychrometric constant [kPa $°C^{-1}$].

There is a large variety of hydrologic models, most based on the conservation of water mass/volume over large areas and on various parameterizations of hydrologic fluxes. The Penman Monteith equation is one of the most advanced resistance based model (Maidment, 1993). This equation makes possible the calculation of evaporation from meteorological variables and resistances, which are related to *stomata* and aerodynamic characteristics of crop. However this equation requires bulky of data sets.

2.5.3 Energy Balance Approach

This approach resembles the water balance approach but in this case its energy balance or budgeting of an evaporation body instead of water flow. The energy balance approach is the current approach that uses sophisticated instruments and remotely sensed data. SEBS (Su, 2003), SEBAL (Bastiaanssen et al., 1998a & b,) and other many are algorithms that have been developed to estimate evaporation by looking at energy balance.

$$R_n = G + H + LE \qquad \text{(Eq. 3)}$$

Where:
’Rn’ is the net radiation,
’G’ is the soil heat flux,
’H’ is the sensible heat flux and
’LE’ is the latent heat flux

The energy budget methods (including the Penman combination methods) are reliable in theory and suitable for research purposes only in small areas, because of their requirements for detailed meteorological data, such as net radiation, sensible heat flux etc. Their practical utility for larger lakes is limited. A major advantage of the energy-balance approach is that it can be used to quantify spatial extent of irrigated fields and their water-use dynamics without reference to source of water as opposed to water balance model which requires knowledge of both magnitude and temporal distribution of rainfall and irrigation applied to fields.

2.6 Use of Remote Sensing in estimation of evaporation

Evaporation is one of important component in the land surface energy balance (Guyot at el, 2008). It is possible to use remote sensors to estimate evaporation because the values of the components of the energy balance equation can be determined with remote sensors. This is because, remote sensors have been designed to measure energy in specific ranges of the electromagnetic spectrum which mostly fall under atmospheric windows at which the atmosphere is almost transparent and atmospheric effect is minimal. There are number of energy balance based methods for estimating the evaporation in instantaneous sensible heat flux which are SEBAL, SEBS, LAS-data, MM5 simulation and other many (Bastiaanssen et al., 1998a, Bastiaanssen et al., 1998b, Su, 2002). Furthermore, the estimation of evaporation using remote sensing enables representative measurements of several hydrological parameters from a scale of few centimetres to the whole globe. Evaporation computed from remote sensors is in instantaneous form. This is a challenge because the water managers are primarily focusing on daily values.

For example SEBAL one of the satellite based method also uses the following equation:

$$R_n = G + H + LE \quad \text{(Eq. 4)}$$

2.6.1 Surface Energy Balance System (SEBS)

This is the method or model for estimating ET developed by Su (2002) which calculates the atmospheric turbulent fluxes and the evaporative fraction using satellite, surface and meteorological information. SEBS consists of remotely sensed data and standard meteorological observations. It is a single-source model (Kwast et al., 2009) which estimates atmospheric turbulent fluxes and surface evaporative fraction from remote sensing data by using several separate modules to estimate the net radiation and soil heat flux and to partition the available energy into sensible and latent heat flux.

The rationale behind the energy balance approach is that evaporation is the change of state of water by demanding supply of energy for vaporization. However, it is mostly affected by difference in land cover types. However SEBS does not take into consideration wind speed and direction which influences atmospheric demand of moisture.

On the other hand, SEBS is capable of estimating sensible heat flux in a same order and magnitude as the field measurement especially when the foot print of the measurement covers one land cover type.

In operation, SEBS requires three sets of data which include remote sensing data like, albedo, emissivity, temperature, and NDVI to derive local surface roughness parameters. It also uses meteorological data collected at the reference height which are: air pressure, wind speed, temperature and relative humidity together with radiation data (downward solar radiation and downward long wave radiation) to compute ET.

This model is based on the conservation of energy principle, where by it considers that all the energy involved in the soil-vegetation-atmosphere interfaces comes from solar radiation, and then expressed as several forms which can be given by Energy Balance Equation as follows;

$$R_n = G + H + LE \qquad \text{(Eq. 5)}$$

Making *LE* the subject:

$$LE = R_n - G - H \qquad \text{(Eq. 6)}$$

Where:

’Rn’ is the net radiation,

’G’ is the soil heat flux,

’H’ is the sensible heat flux and

’LE’ is the latent heat flux, the measure of evaporation, but neglecting the energy needed for photosynthesis and heat stored in the vegetation.

i. NET RADIATION

Net radiation is the sum of total incoming shortwave radiation and outgoing long wave radiation at the Earth’s surface.

Net radiation is expressed in the equation below:

$$R_n = (1-\alpha)K\downarrow + \varepsilon.L\downarrow - L\uparrow \qquad \text{(Eq. 7)}$$

Where: R_n is Net Radiation, K↓ incoming shortwave radiation measured at the weather station, $L\downarrow$ and $L\downarrow$ are incoming and outgoing wave radiation respectively α is the surface reflectance and ε is surface emissivity.

$$L\downarrow=\sigma..\varepsilon_a.T_a^4 \quad \text{(Eq. 8)}$$

Where:

σ is the Stephen Boltzman constant 5.67×10^{-8} $Wm^{-2}k^{-4}$

ε_a is emissivity of air by (Campbell and Norman, 1998)

But,

$$\varepsilon_a = 9.2.10^{-6}.(\Gamma_a + 273.15)^2 \quad \text{(Eq. 9)}$$

Now,

Γ_a = air temperature at the reference height

$$\text{L (out) or } L\uparrow = \varepsilon_s \sigma T_s^4 \quad \text{(Eq. 10)}$$

$\varepsilon_s\, and\, \mathrm{T}_s$ are surface emissivity and time respectively.

ii. SOIL HEAT FLUX

Soil heat flux equation is as follows;

$$G_o = R_n.[\Gamma_c(1-f_c).(\Gamma_s-\Gamma_c)] \quad \text{(Eq. 11)}$$

$\Gamma_c = 0.05$ for full vegetation canopy by Monteith cited in Su et al., (2001)

Γ_s =0.315 for bare soil (Kustas and Daughgtry; 1989)

iii. SENSIBLE HEAT FLUX

SEBS recognizes the two extremes which either favors or limits evaporation. The limits are the wet limit H_{wet} and sensible heat flux at the dry limit H_{dry}.

Now the dry limit is given as;

$$H_{dry} = R_n - G_o \quad \text{(Eq. 12)}$$

The above equation means, evaporation is zero due to the limitation of soil moisture

$$H_{wet} = R_n - G_o - \lambda E_{wet} \approx 0 \quad \text{(Eq. 13)}$$

The above when combined to PENMAN MONTEITH equation it gives us Sensible heat flux at wet limit as follows;

$$H_{wet} = \left[\frac{\left[(R_n - G_o) - \frac{\rho c_p}{r_{ew}} . \frac{e_s - e_a}{\gamma} \right]}{1 + \frac{\Delta}{\gamma}} \right] \quad \text{(Eq. 14)}$$

Where:

e: is actual vapour pressure measured

e_s: the saturation vapour pressure

γ : is Psychrometric constant

Δ : is the rate of saturation

r_{ew}: external resistance

$$r_{ew} = \frac{1}{kn_*} \left[\ln\left(\frac{z-d}{z_{oh}} \right) - \psi_h \left(\frac{z-d}{L_w} \right) + \psi_h \left(\frac{z_{oh}}{L_w} \right) \right] \quad \text{(Eq. 15)}$$

$$L_w = - \frac{\rho . u_*^3}{kg.0.61.(R_n - G_o)} / \lambda \quad \text{(Eq. 16)}$$

λ is latent heat of vaporization = 2.45MJ kg^{-1}

SEBS has been validated under a wide range of environmental and climatologically conditions; it was tested versus AET rates in a semiarid inland basin in NW China (Li, 2001; Su et al., 2003a), and for drought disaster monitoring (Su et al., 2003b). It was evaluated well as compared with other remote sensing techniques over irrigated fields (Kustas and Norman, 1999; Su et al,. 2001, Su, 2003, Su et al., 2007). More recently, validations of SEBS have been reported by (Su et al 2005, 2007) using data from the SMACEX experiment and CEOP references sites. However SEBS has not been used in the Wami Basin neither at Mkindo catchment thus the essence of the research.

SEBS for ILWIS helps in processing the satellite images and results are; maps of net radiation, latent, sensible and soil heat fluxes, evaporative fraction, instantaneous and daily AET, and complementary files as standard outputs.

3.0 DESCRIPTION OF THE STUDY AREA

3.1 Physiography

Mkindo catchment is located at the Northern end of Morogoro region between 5° to 9° S Latitudes and 36° to 40° E longitudes[1]. The Mkindo River is one among the big rivers draining directly into the Wami basin. The study was narrowed down to catchment level instead of studying the whole basin which approximately covers 33,000 km^2, to cater for time and resources limitation. Mkindo catchment covers an area of 1006 km^2 located within Mvomero district (Nnunduma, 2005). Figure 3.1 below shows the map of Mkindo catchment as part of Morogoro region and Wami River Basin.

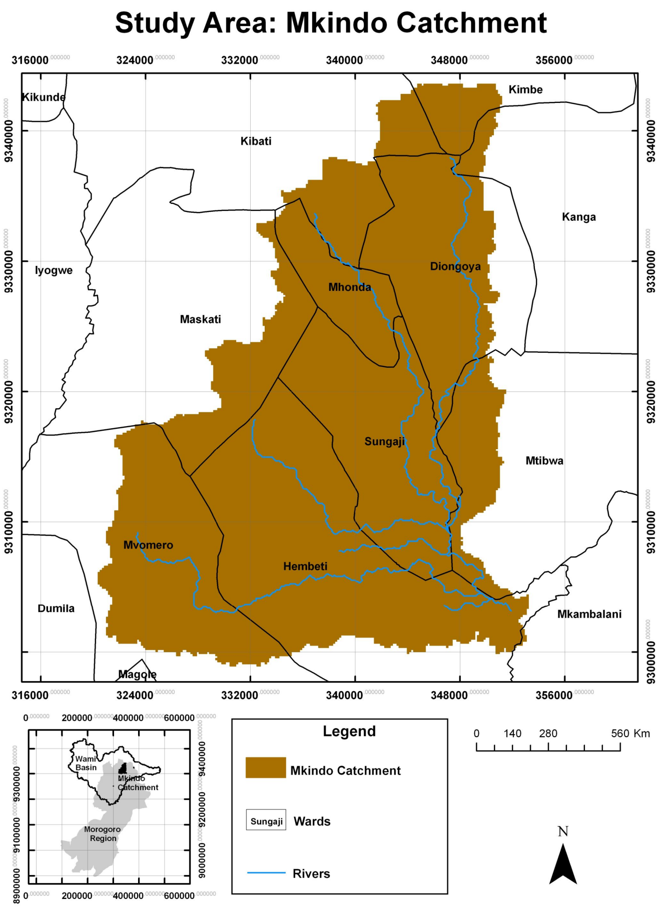

Figure 3.1 Mkindo Catchment in the Wami-Ruvu Basin

[1]http://www.googlearth com

The long term average maximum and minimum temperature at the Mkindo catchment is 32°C and 20°c respectively. The headwater of the catchment is under forest reserve. The topography of the catchment varies, with the Nguru Mountains on the upper parts of the catchment and relatively gentle slopes on the lower parts. The elevation of the catchment ranges from 2200masl on the upper part to 360m at the foothills (Mkindo village) and 340m at the confluence with the Wami River. Figure 3.2 shows the soil map, the soils vary across the topo-sequence, with well drained sandy soils on the upper parts while loamy and black cotton clay soils dominating the middle and lower slopes.

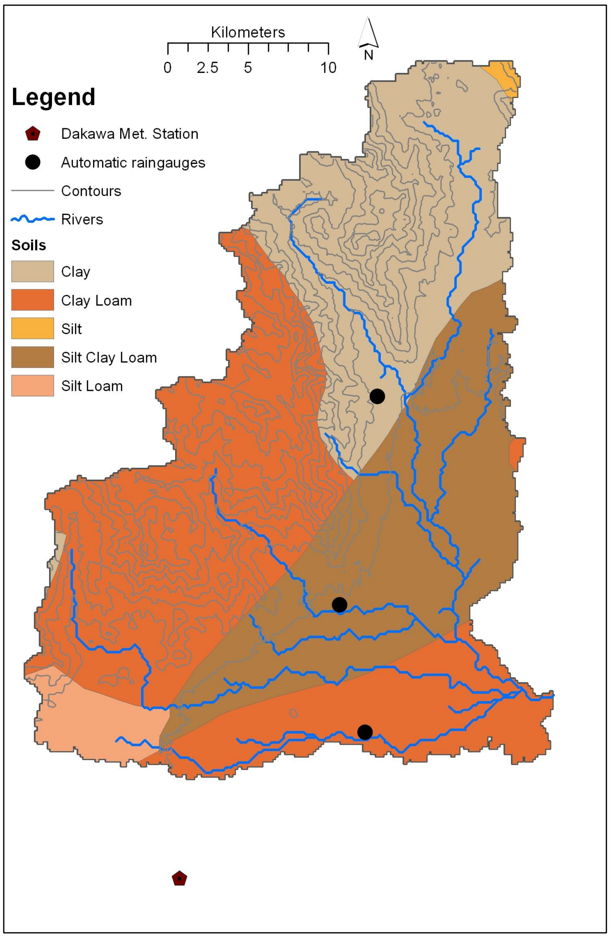

Figure 3.2 The Mkindo soil map

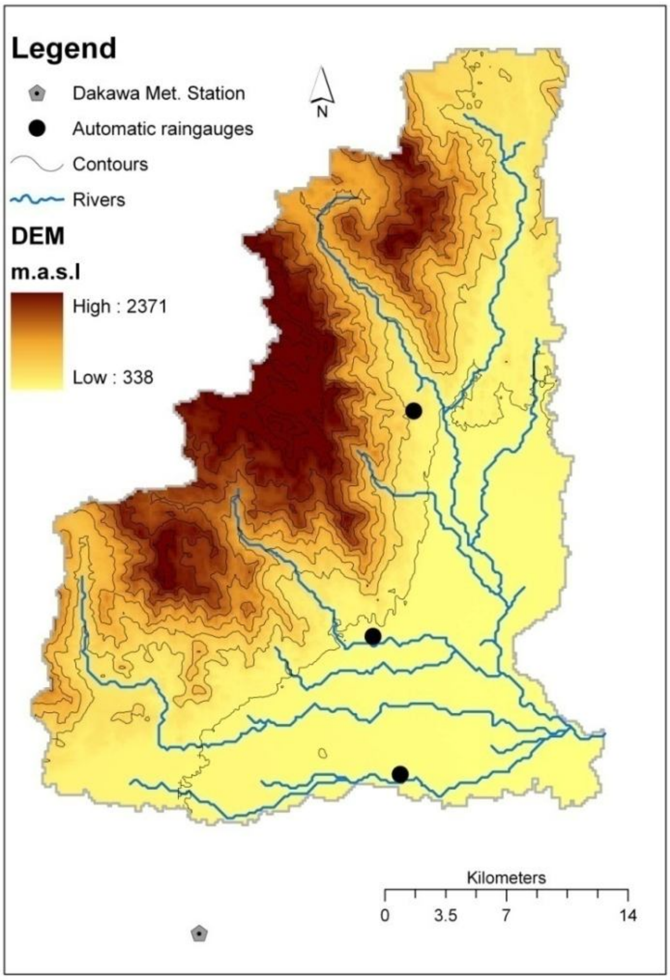

Figure 3.3 DEM map and the distribution of Meteorological and gauging stations

The rapid change in elevation (from 2371 to 360m) and subsequent gentle slope (from 360 to 338 m) as clearly shown by Figure 3.3, has resulted in undulating river network on the lower slopes, with permanent wetlands on the lower parts of the catchment. The main rivers draining the catchment are the Mkindo and Diwale, with the latter ultimately draining into the Wami River. Recently, the Stockholm Environment Institute through the Agriculture Water Management solutions project installed a gauging station in the Mkindo River as shown by Figure 3.3 with water levels being recorded three times a day.

Figure 3.4 River Gauging Station in the Mkindo River

3.2 Water Resources Development

The Mkindo catchment is endowed with substantial water resources, with several perennial streams flowing from the Nguru mountains, which ultimately feeds into the Wami River. Most of these streams flow into wetlands on the lower slopes of the catchment before draining into the Diwale River, a main tributary of the Wami River. There is no literature on water resources in the catchment. This could be attributed to the fact that there is no hydrological monitoring network in place and the challenge associated with the complex drainage pattern especially on the middle and lower slopes of the catchment. The significance of the wetlands in the hydrology of the catchment needs to be understood well, notably the total evaporative flux which is a main component of the water balance in sub-Saharan Africa.

There are numerous wetlands in the middle slopes which serve as growing areas of mainly rice crop and hence making it a challenge to quantify the water resources of the catchment. Unfortunately there is no available literature on water resources in or around the Mkindo catchment and hence capital investment is required in hydrological monitoring if a detailed analysis of water balance is to be done. The Government of Tanzania has developed several policies and strategies in the Agricultural sector in order to achieve food security and economic development and most of these policies have emphasized the role of irrigation in as a key element in food production in rural areas due to rainfall variability.

The Mkindo catchment has a 150 hectare smallholder irrigation scheme, the Mkindo irrigation scheme, with the main crop being rice. Maize crop is occasionally grown on minor scale for household consumption, while the rice crop is the main cash crop.

Figure 3.5 The intake structures of the Mkindo Irrigation Scheme

Figure 3.6 Rice fields in the Mkindo irrigation scheme

3.3 Land Uses

The main land uses in the Mkindo catchment are:

i) Smallholder irrigated farming
ii) Smallholder rain-fed farming
iii) Commercial sugar cane farming
iv) Forestry
v) Livestock grazing

Commercial sugar cane farming is mainly on the eastern parts of the catchment close to the Mtibwa sugar factory. A Forest reserve occupies close to a 1/8th of the catchment and the local communities are allowed, with permission, to use the forest for medicinal and other household purposes (Villagers).

4.0 MATERIALS AND METHODS

4.1 Data Acquisition

Estimation of Evaporation was done based on cloud free MODIS level 1B data with pixel size 1km × 1km which were downloaded from NASA website called LAADS web. Generally the process of downloading data involved search for the clear pixels of the study area taken by AQUA satellite which normally passes over East Africa at 12:00HRS noon. Figure 4.1 shows an interface of searching page when acquiring the images.

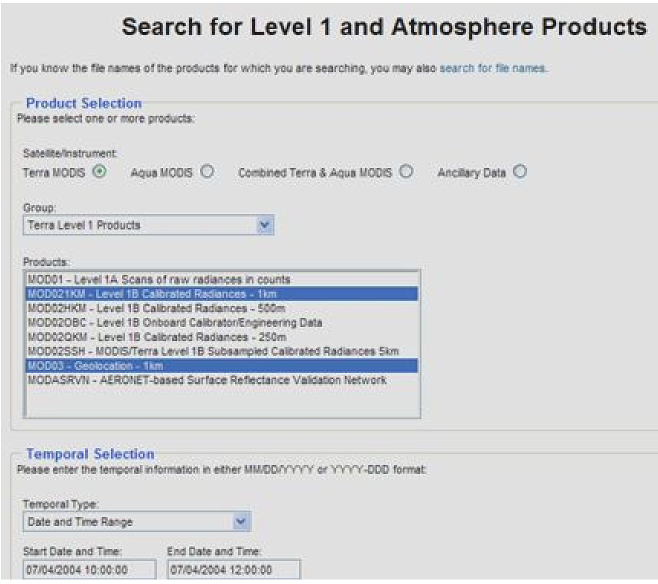

Figure 4.1 Searching

Moderate-resolution Imaging Spectroradiometer (MODIS) is one of the primary land observation sensors on-board the TERRA (EOS AM) and AQUA (EOS PM) satellite. Terra's orbit around the Earth is timed so that it passes from North to South across the Equator in the morning, while Aqua passes south to north over the Equator in the afternoon. Both MODIS satellites view the Earth in every 1 to 2 days taking images in 36 spectral bands.

Aqua level 1B products were used which means it is raw data in 1 km calibrated radiance taken in number of bands. MODIS Level 1B images are geo-located and stored in 16 bit scaled integer with associated calibration parameters and other information in hierarchical data format. Reflectance scale and reflectance offset for relevant reflective solar bands (1 and

2) and radiance scales and radiance offsets for both relevant reflective and thermal emissive bands (31 and 32) were extracted using hierarchical data format (HDF) explorer.

Advantages of using AQUA MODIS over sensors like NOAA/AVHHR; are that it has improved spectral and radiometric resolution compared to older sensors, also, AQUA has atmospheric sounding sensors such as (AIRS/AMSU) providing atmospheric temperature or vapor that can be optionally combined with standard MOD 16.

Moreover, in combination with Terra/MODIS, the time resolution of the ET observations overland can be increased.

Because the use of MODIS images for Surface Energy Balance model required that the parameters like emissivity, albedo, surface temperature, surface reflectance and vegetation index to be included. MODIS data or products were downloaded free of charge from[2]. The tables 4.1 and 4.2 respectively show the time, dates, month and year of the downloaded images and bands in each of the image.

Table 4.1 Data acquired

No.	*Date*	*Time of capture*
1	30th June 2008	11:20 Hrs
2	6th September 2008	08:00 Hrs
3	9th September 2008	11:25 Hrs
4	25th October 2008	11:35 Hrs
5	28th July 2009	11:15 Hrs
6	25th September 2009	08:00 Hrs

[2] http://ladsweb.nascom.nasa.gov/data

Table 4.2 Bands

Band	*Spatial resolution (m)*	*Wavelength (micron)*	*Band type*
1	250	0.645	Reflectance
2	250	0.866	Reflectance
3	500	0.470	Reflectance
4	500	0.555	Reflectance
5	500	1.24	Reflectance
6	500	1.64	Reflectance
7	500	2.13	Reflectance
31	1000	11.03	Emissive
32 2	1000	12.02	Emissive

4.2 Data Processing and Bio-Physical Parameters Estimation

4.2.1 Reprojection and converting MODIS level1B data

The MODIS L1B data were in swath format which needs to be converted to format which is compatible with GIS software like ILWIS which was used in this research. To re-project MODIS data, the author used MRTSwath tool as shown in Figure 4.2 and HDFView software Figure 4.3 to convert the MODIS level-1B data into GeoTIFF.

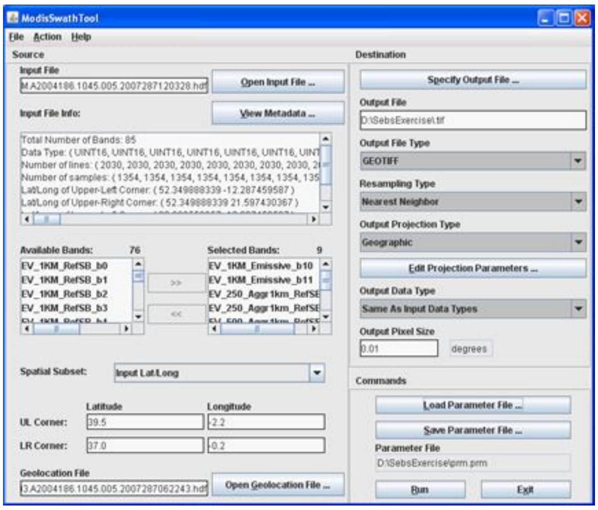

Figure 4.2 Converting desired channels in the given MODIS level-1b file into GeoTIFF

4.2.2 Importing images into ILWIS

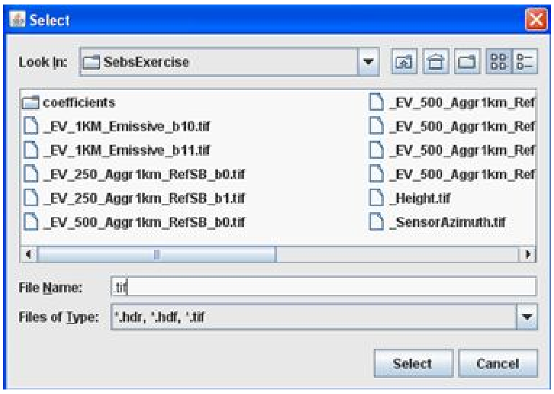

Figure 4.3 Importing GeoTIFF into ILWIS raster files.

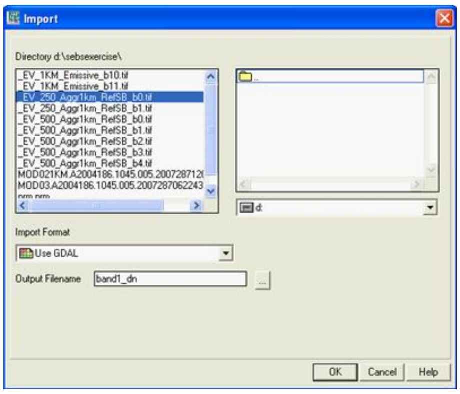

Figure 4.4 Importing MODIS bands into ILWIS screen

4.2.3 Pre-processing for SEBS

1. Raw to radiances/reflectance (MODIS)

The MODIS Level 1b data are given in SI (simplified number); therefore, the images were converted to reflectances and radiances as shown by Figure 4.5 and Figure 4.6 respectively. MODIS channels 1 to 7 were converted to reflectances and channels 31 and 32 were converted to radiances.

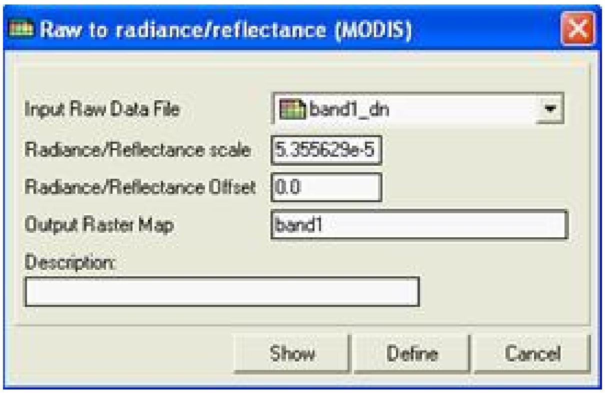

Figure 4.5 Converting band1 into reflectance dialog box

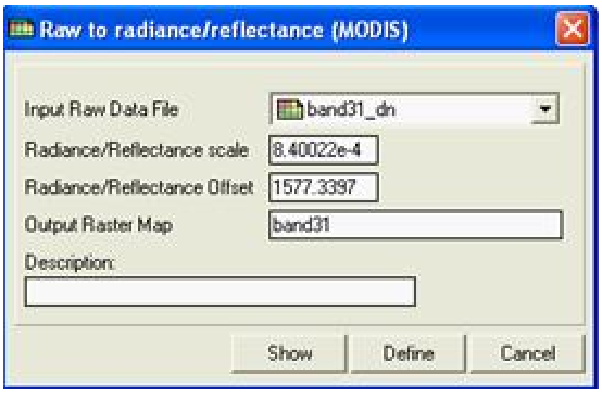

Figure 4.6 Converting band31 into radiances dialog box

The SEBS in ILWIS provides the tools to convert the imported MODIS channels in digital number /simplified integer into radiances or reflectance, which is done by applying the proper calibration coefficients. The calibration coefficients consist of a scale and offset and are provided in the HDF header file. Figure 4.7 is an illustration of the HDFView interface.

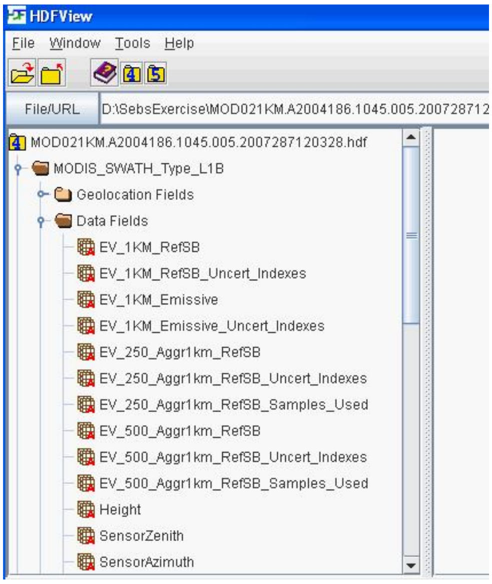

Figure 4.7 HDF View

This action was followed by brightness temperature computation, SMAC for atmospheric correction, surface albedo computation, surface emissivity, NDVI and surface temperature computation.

2. Brightness computation

This process involves converting the bands 31 and 32 of MODIS from radiances to blackbody temperatures which is done by applying Planck equation:

$$T_c = \frac{c_2}{\lambda_c \log\left[\frac{c_1}{\lambda_c^5 \pi L_s} + 1\right]} \qquad \text{(Eq. 17)}$$

where: $T_C =$ brightness temperature, from a central wavelength

$\lambda =$ the sensor's central wavelength

3. Atmospheric Correction (SMAC)

SMAC is a tool for atmospheric effect correction of the visible and near visible bands of different satellite sensors like MODIS and others, in this research the algorithm by (Rahman et al, 1994) was used. The atmospheric correction was performed for bands 1 to 7, but each band separately from the other. The Atmospheric correction procedure called for the use of Aerosol Optical Depth 550 micrometer which was obtained from[3] and also ozone content which was retrieved from[4]

4. Surface albedo

Surface albedo is the ratio of reflected to incident solar radiation at the earth's surface and is a critical variable affecting the earth's climate (Cess, 1978). In semi arid regions, an increase in albedo leads to a loss of radiative energy absorbed at the surface, and convective overturning is reduced (Liang et al.., 2001). Wu et al., (2006) indicated that the reflectivity of a surface is wavelength dependent, with few natural surfaces being uniform reflectors across portion of the electromagnetic spectrum of interest. Using MODIS bands 1, 2, 3, 4, 5, and 7, the formula by Liang et al., 2003 was used:

$$\alpha = 0.160\mu_1 + 0.291\mu_2 + 0.243\mu_3 + 0.116\mu_4 + 0.112\mu_5 + 0.018\mu_7 - 0.0015 \qquad \text{(Eq. 18)}$$

where: μ_i is the reflectance of the respective band.

α = albedo

5. Surface emissivity

The ratio of the thermal energy radiated by the earth's surface to the thermal energy radiated by a black body at the same temperature, i.e., surface emissivity (e), was computed using the relationship indicated in the equation:

$$\alpha = 1.009 + 0.047\ln(NDVI) \qquad \text{(Eq. 19)}$$

Where;

α = albedo

[3] http://aeronet.gsfc.nasa.gov

[4] http://jwocky.gsfc.nasa.gov

It should be noted that this method is applicable in the NDVI range of 0.16 to 0.74. This equation is hence not valid for water bodies with negative NDVI values. Therefore, the water bodies were masked and constrained to an emissivity value of 0.999.

6. Normalized Difference Vegetation Index (NDVI)

The Normalized Difference Vegetation Index (NDVI) is commonly used to provide information on vegetation density, color of surface and cultivation practice due to the property of the chlorophyll, which strongly absorbs radiation in the red parts of the electromagnetic spectrum and reflects it in the near-infrared part (Farah and Bastiaanssen, 2001). NDVI was computed using the difference in reflectance in the red and near infra-red region of the spectrum as indicated in the equation by Sobrino, 2003:

$$NDVI = \frac{\mu_2 - \mu_1}{\mu_1 + \mu_2} \qquad \text{(Eq. 20)}$$

where: μ_1 and μ_2 are the spectral reflectances of bands 1 and 2, respectively.

In addition, a vegetation proportion Pv was calculated using the following formula:

$$\mathrm{P_v} = \left(\frac{(NDVI - NDV\,\mathrm{Im}\,in)^2}{(NDV\,\mathrm{Im}\,ax - NDV\,\mathrm{Im}\,in)^2} \right) \qquad \text{(Eq. 21)}$$

Where: NDVI max=0.5 and NDVI min= 0.2

Atmospherically corrected surface reflectance maps were used.

7. Surface temperature

The land surface temperature was computed (using a split window method) from the radiant temperature, which was obtained after atmospheric correction of the brightness temperature using the surface emissivity as highlighted in Tasumi et al., (2000). The brightness temperature was derived from the thermal bands (31 and 32) through the inversion of the Plank’s function as indicated in Equation:

$$T_r = \frac{C_2}{r \ln\left[\frac{C_1}{\pi r^5 B_r} + 1 \right]} \qquad \text{(Eq. 22)}$$

where: T_r is the bands brightness temperature $(^{\circ}K)$ and C_1 and C_2 are constants r is the respective wavelength (μm) and B_r is the radiance value (W.m^{-2} steradian^{-1}).

The accurate estimation of land surface albedo and land surface temperature is essential because they determine the absorption of radiation energy by the land surface.

After computation of land surface temperature the Author ran the SEBS model, Figure 3.14 shows the SEBS interface. SEBS operation derived the radiation balance components, turbulent heat fluxes, evaporative fraction and evapotranspiration using remote sensing observation data in combination with the meteorological measurements.

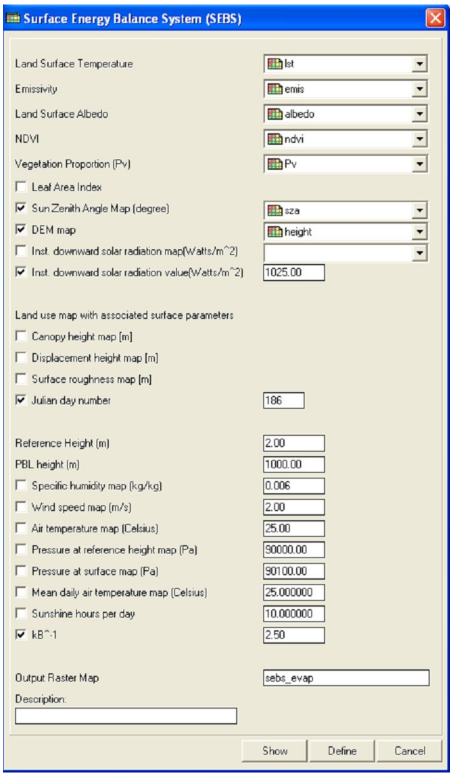

Figure 4.8 The SEBS interface

The evaporative water uses of different land uses/covers were then estimated in the Mkindo Catchment at different spatial and temporal scales from *ET* images derived from SEBS model. Interested in the total evaporation in the months images acquired, computation of the monthly *ET* was carried out by extrapolating the SEBS results within a particular month. The monthly *ET*, ($ET_{monthly}$), was then computed using an equation by (Bastiaanssen, 1998);

$$ET_{Monthly} = \sum_{i=1}^{i=n} \left(ET_{SEBS}\right)_I \left(K_m\right)_i \qquad \text{(Eq. 23)}$$

ET_{SEBS} is daily *ET* image and K_m is a multiplication factor for the representative period while *n* is the number of *ET* images processed in the respective month.

The procedure of calculating multiplication factor (*Km*) involves determining the ratio of the cumulative reference *ET* to the average reference *ET* over the period. Table 3.3 and 3.4 respectively shows the multiplication factor values for the months in 2008 and 2009.

Table 4.3 Multiplication factor for months in 2008

Date	*30-Jun*	*6-Sep*	*9-Sep*	*1-Oct*
Cumulative ET_r for the month	45	98	83	83
ET_r on image date	1.147	3.846	3.254	3.304
K_m	39.2	25.5	25.5	25.1

Table 4.4 Multiplication factor for months in 2009

Date	*28-Jul*	*25-Sep*
Cumulative ET_r for the month	82.4	82.8
ET_r on image date	3.7	3.217
K_m	22.3	25.7

The meteorological data which were initially in hourly step were converted to daily step purposely to feed them on the work spread sheet for daily Penman-Monteith.

The monthly *ET* maps were used hence giving a picture of the monthly water consumption of different land uses/cover.

4.3 Land Cover/Use Map Making

Land cover map used was extracted from the Africa cover map that were made and tested by ESA/ESA Globcover Project led by MEDIAS-France/Postel which was made in 2006 and upgraded as per ground truthing. ENVI software ArcGIS 9.0 and Arc View 3.2 were used during the process of land cover map making.

4.4 Relationship between Evaporation and Land cover

Normally for evenly distributed data sets, Analysis of Variance (ANOVA) test is used to statistically test if there is a significant difference between variables, in this case to nullify the null hypothesis that states that there is no difference in evaporation among different land covers ANOVA test was carried out using S^+ software. To test whether there is difference between the mean evaporation values of the SEBS modeled results and those calculated Potential evapotranspiration, Wilcoxon test was carried out. Wilcoxon test was chosen because the nature of the data in this case was not evenly distributed.

Surface Energy Balance System (SEBS) model required some meteorological data sets, the time series meteorological data set from March 2008 to December 2009. From Wami Prison meteorological station the following meteorological data were collected; temperature, rainfall, wind speed and direction, relative humidity, air pressure and radiation, though this station is outside Mkindo sub catchment due to fact that weather stations of the standard of recording the required parameters were not available within the study area. Distance from the stations and the study area was within the range that can be accommodated by the model. Data were provided on an hourly basis though the satellite images are instantaneous and thus some extrapolations and conversions had to be carried out.

Figure 4.9 Mkindo Automatic Meteorological Station

Using ILWIS 3.0 which is equipped with the SEBS model, the SEBS operation was carried out and managed to derive the radiation balance components, turbulent heat fluxes, evaporative fraction, and evapotranspiration using the remotely sensed images and meteorological measurements. The results from running the SEBS gave instantaneous and daily evaporation results.

Furthermore, the SEBS results obtained were proofed using the Potential ET computed using Savage MJ, 2007 (A work spread sheet for daily Penman-Monteith grass reference evaporation from a minimum set of meteorological data.)

5.0 RESULTS AND DISCUSSION

5.1 Results

5.1.1 Spatial Distribution of total Evaporation in the Mkindo Catchment

Figure 5.1 shows the spatial distribution of SEBS model derived total evaporation in the Mkindo sub catchment in June and September 2008. The monthly values of total evaporation in June show a range from 34mm/m to 98mm/m. Relatively high evaporation is observed in small patches of the sub catchment especially at the lower part of the catchment.

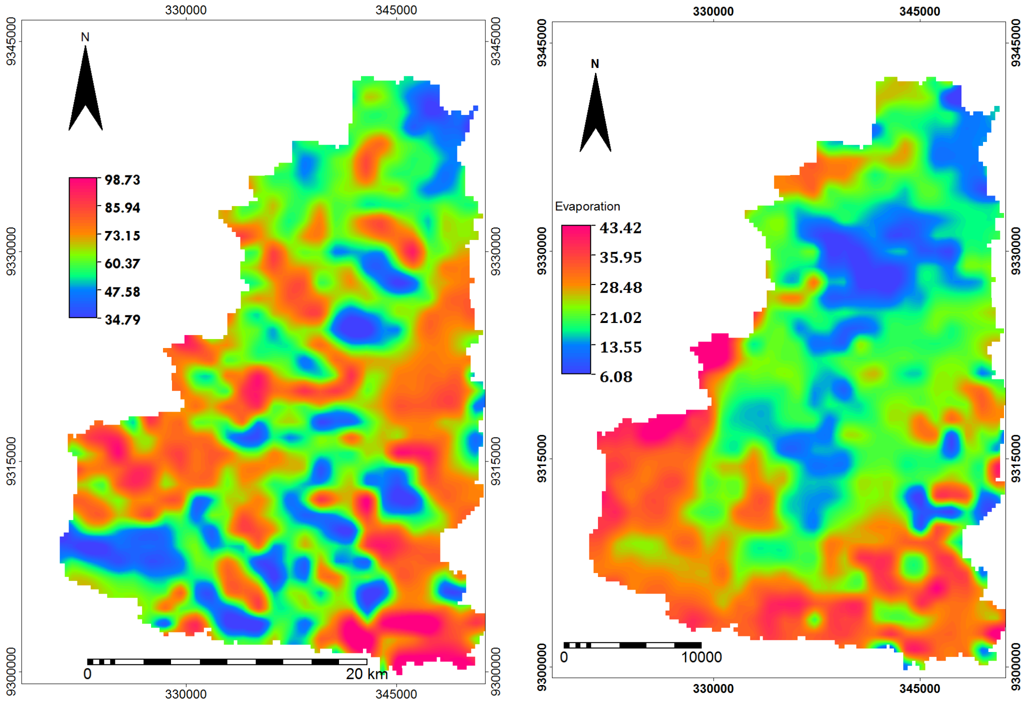

Figure 5.1 Spatial Variation of total monthly Evaporation in (left) June 2008 and (right) September 2008

On the other hand, the monthly values of total evaporation in September ranges from 6mm/m to 43mm/m. Relatively high evaporation is observed in the lower parts of the catchment.

The September map shows that the spatial distribution of the total evaporation has a slight shift to lower values with a minimum of 6mm and maximum of 43mm. It is also been observed that wind speeds are higher during "*Kipupwe*" a season of high winds, ranging from

12m.s^{-1} and above while in June they are around 4m.s^{-1}. However, it is observed that, the general spatial distribution of total evaporation is maintained with the lower part of the catchment experiencing relatively higher evaporation values compared with other parts of the catchment.

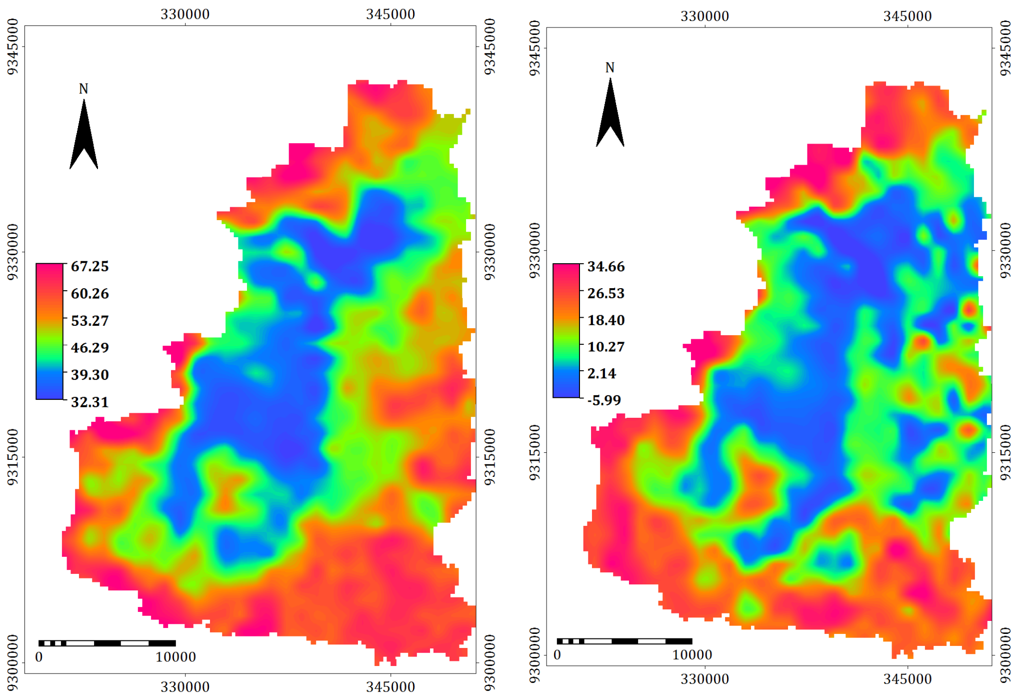

Figure 5.2 Spatial Variation of total monthly Evaporation in (left) July 2009 and (right) September 2009

Figure 5.2 shows the total evaporation for July and September 2009. It can be observed that, spatial distribution of evaporation has created three clear layers. High values can be observed on the outer layer of the catchment area followed with a second layer of relatively low values as you penetrate towards the middle of the catchment. The third layer is found at the mid part of the catchment with lowest evaporation values.

The highest value of evaporation in July is 67mm, there is dropped down of the evaporation values in September when compared to evaporation values of July 2009. Values in September range from 3mm to 34mm while those of June range from 32mm to 67 mm.

It is therefore clear that, in the Mkindo catchment the spatial distribution of total monthly evaporation varies with accordance to heterogeneity of the landscape as well as the distribution of land covers. The areas in the map which are blue are areas with the lowest evaporation values and the areas with pink are the areas which have the highest values. It is clear and evident that the evaporation values are higher on the lower parts of the catchment on all the four months results. The mid part has got the lowest values during the four studied months.

5.1.2 Differences in evaporation among different Land Use/ Cover types

Spatial distribution of the land use/cover

The land cover/use map of 2006 of the Upper-Wami Basin shows that 50% of the basin is covered by forests both Evergreen and Deciduous Forests. Agricultural land accounts for 30% of the total Mkindo catchment area. Shrub land and grass land accounts for the rest area in the catchment.

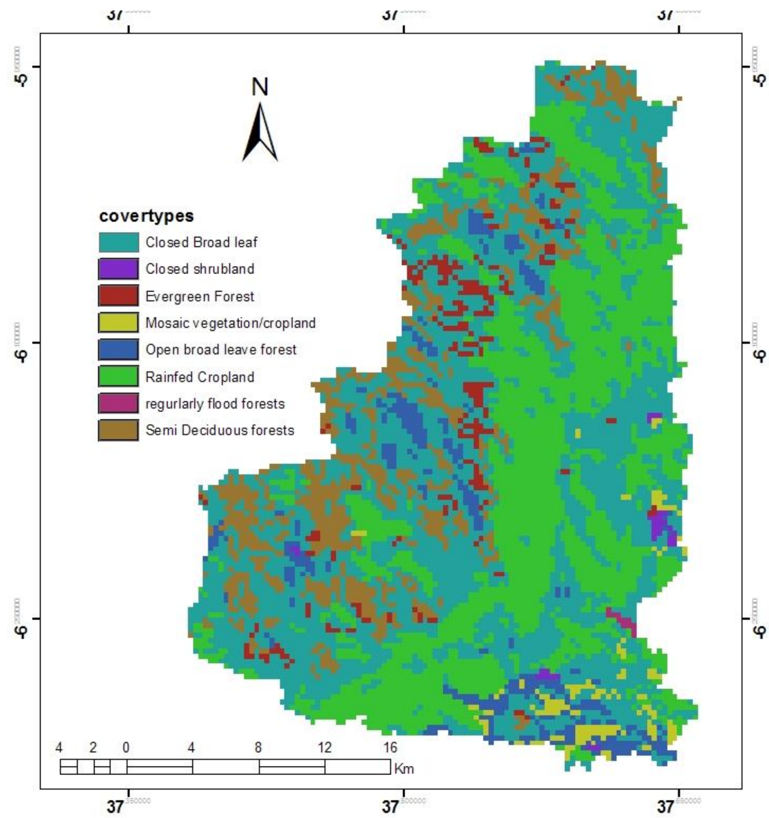

Figure 5.3 Spatial Distributions of Land Cover/Uses

Contribution of Land Cover/Use to total Evaporation

Results of evaporation among different land cover types are illustrated in figure 4.4. The evergreen forests have the highest mean evaporation values 85mm followed by the open broad leaved deciduous forest with mean of 63mm. The rain fed crop has the least mean value of 60mm because of the dry spells which are normally experienced at the Mkindo catchment. ANOVA results show that, there is significant ($p<0.05$) difference of mean evaporative water use.

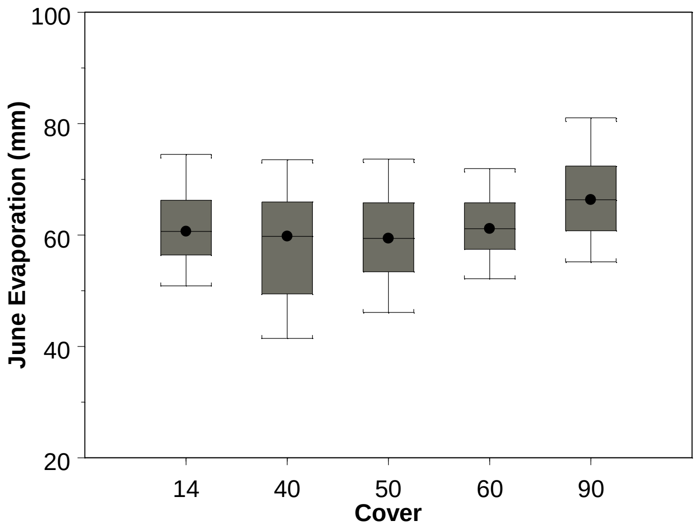

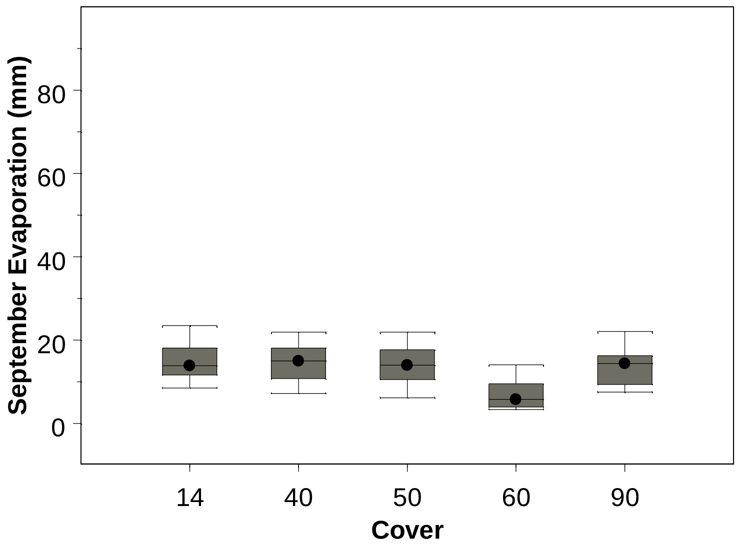

Figure 5.4 Box plots showing the statistical distribution of June and September 2008 Evaporation by Land cover/use **(14= Rain fed croplands, 40=semi deciduous forest, 50=closed broad leaved deciduous forest, 60=open broad leaved deciduous forest, 90=evergreen forest).**

Also, figure 5.5 represents the statistical distribution of evaporation by land cover/use for July 2009. It is observed that the statistical distribution of the total evaporation in July 2009 is so varying. In this case Semi Deciduous Forest has the highest mean value, but the quartiles trend is the same, the Evergreen Forest having the highest upper quartile value. There is a significant ($p>0.05$) difference in the evaporative water uses with accordance to land uses/covers.

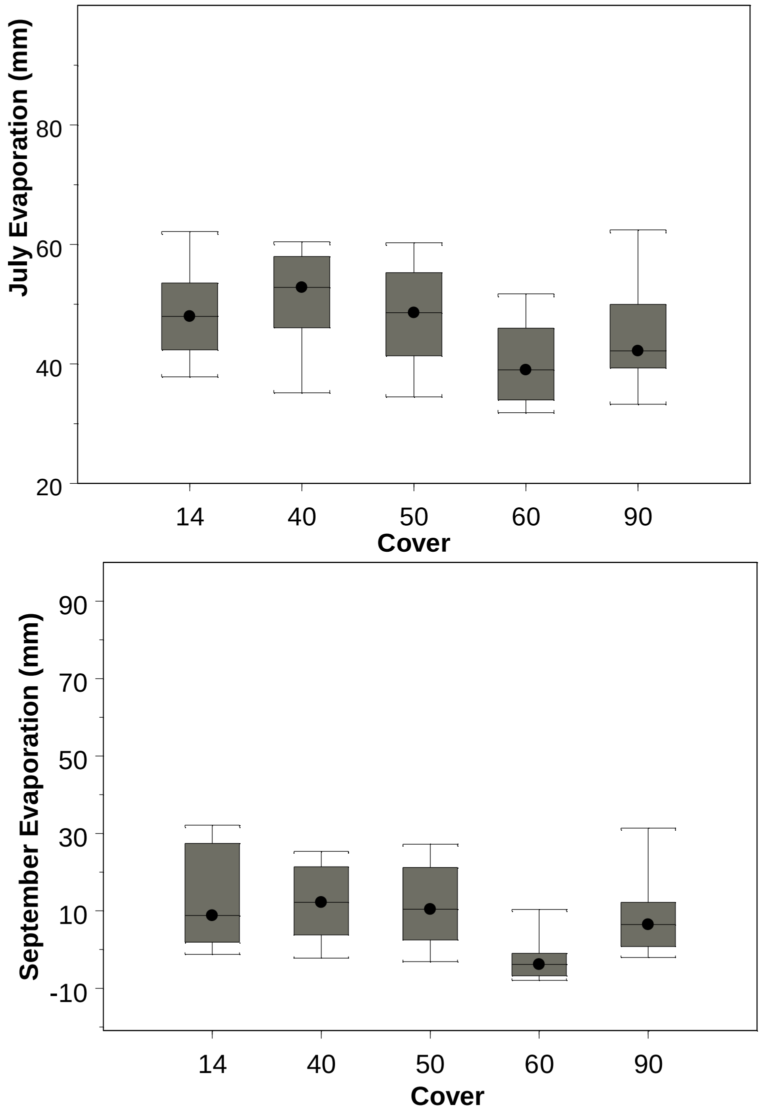

Figure 5.5 Shows the statistical distribution of July and September 2009 Evaporation by Land cover/use **(14= Rain fed croplands, 40=semi deciduous forest, 50=closed broad leaved deciduous forest, 60=open broad leaved deciduous forest, 90=evergreen forest).**

Rain fed cropland consuming highest value of around 35mm during September 2009. Open broad leaves forest have the lowest value. The average evaporation value is high for semi deciduous forest.

5.1.3 Comparison of SEBS Modeled evaporation and calculated evaporation

Figure 4.6 shows comparison of the SEBS derived daily evaporation values for cloudy free days and the calculated Potential Evapotranspiration (*ETo*). It can be observed that there is good agreement between the daily evaporation values of the month of June and October 2008. The ET_o values are slightly higher than SEBS results except for October 2008 where SEBS results has higher values than the results of calculated Potential Evapotranspiration.

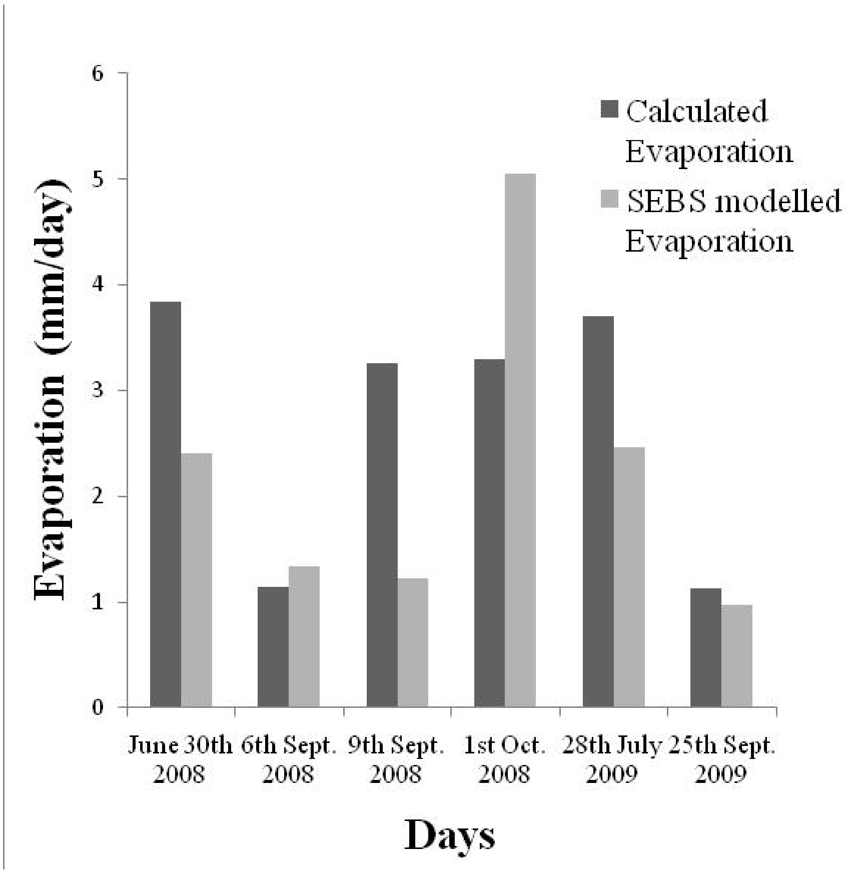

Figure 5.6 Comparisons of SEBS and Potential *ET*

Figure 5.7 illustrates statistically whether there is significant difference between the results of evaporation derived form SEBS model and those of calculated Potential Evapotranspiration. Wilcoxon tests show that there is no significant different between median of *ETo* and that of SEBS derived evaporation.

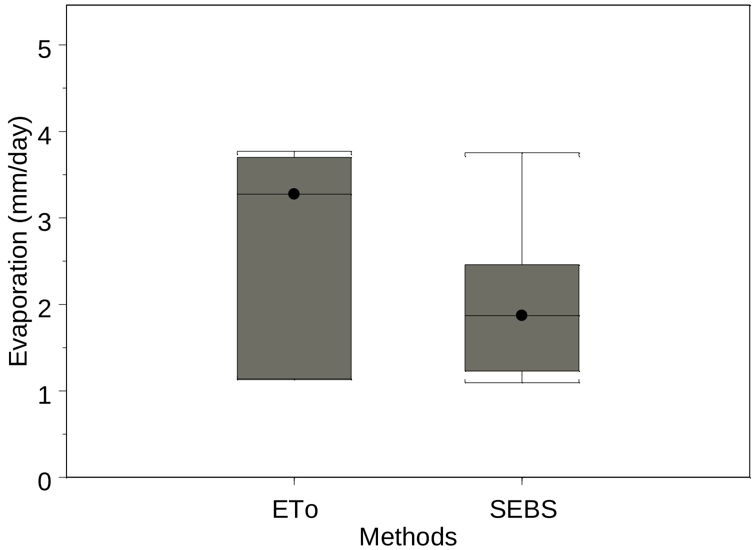

Figure 5.7 No significant difference between modelled SEBS mean evaporation (SEBS) and calculated Evaporation (ET_o) (Wilcoxon test, p = 0.5887,n =6)

5.2 Discussion

Results have indicated that, there is a spatial and temporal variation of total evaporation over the Upper-Wami Basin. During the month of June 2008 as indicated by figure 5.1 most parts of the Mkindo catchment appears to have bare land and or burnt spaces and hence low evaporation values. However the evaporation values generally are relatively high reaching 98mm.month. In September total evaporation is relatively low, upper most value being 43mm for September 2008 and 34mm for September 2009. The study therefore, conforms to existing knowledge that evaporation is a continuous variable varying with time (Kwast et al., 2009), (Kongo, 2008), (Lin, 2006), (Mohamed et al., 2004), (Farah et al., 2004). Also, the results have shown that the evaporation distribution pattern is spatially continuous, in Figure 5.2, the lower parts of the catchment has been observed to have the highest values of evaporation and I discovered that the reason for that is, the lower parts of the catchment has permanent wetlands which means availability of water is not a limit to evaporation in this lower part of the catchment. Due to the fact that evaporation varies with time and space the SEBS model method which uses satellite images is relevant.

Furthermore, the results suggest that there is a difference between the evaporative water uses for different land uses/covers. The Evergreen Forests tend to continue transpiring throughout out the year and having the relatively high average evaporation values when compared to other land covers/uses like Deciduous Forests which tend to adapt to availability of water, with less transpiration and shedding of leaves during the dry season to cope with the water stress. These findings are supported by other findings by (Legesse, 2003), in Ethiopia who specifically found that land cover change has different responses to hydrological cycle. Also, (Hemakumara et al, 2003) they realized that different vegetations transpire differently meaning each land cover type has its own evaporative water use.

Finally, the results showed statistically there is no significant difference between SEBS modeled Evapotranspiration results and the calculated Potential Evapotranspiration. Whereby, it can be deduced that SEBS is not only an objective estimator but it has an added advantage of being spatially continuous. However, though the statistically there is no significant difference in figure 5.6 the graph of comparison shows that in October 2008 there is a remarkable difference between modeled and calculated, SEBS results having very high values when compared to calculated. This may have been caused by errors when running the model, but the other reason may be an error when calculating.

Nevertheless, it must be cautioned that the study had a few limitations and challenges. One, data availability from automatic gauging stations for validating SEBS estimates was limited because of high expenses. For instance, this study depended on 1 automatic gauging station for the estimation of ET_o, although it had been planned to use 3 automatic meteorological stations. Also, MODIS images are free but have a low spatial resolution of approximately 1km which results in errors concerning the area of different land cover types, particularly those that cover relatively small areas.

6.0 CONCLUSION AND RECOMMENDATIONS

The main objective of carrying this study was to test whether there are significant differences in evaporation among different land cover types in Mkindo catchment based on MODIS satellite estimates. It is therefore concluded that;

1. Evaporation significantly varies among different vegetation types at different times of the year.

2. The median SEBS derived evaporation does not significantly differ with the median calculated evaporation, a good agreement between the SEBS modeled evaporation results and calculated Potential Evapotranspiration verifies that SEBS is a useful and accurate tool to estimate the evaporative water uses for different land covers/uses but the SEBS evaporation estimates having an added advantage because it is spatially continuous.

3. The results indicate that SEBS could be used as an important method for estimating evaporation values for the purpose of water balance modeling.

It is also recommended that;

1 Improved evaluation of the SEBS model could be conducted with an increased number of Automatic Meteorological station with capability of recording all important meteorological parameters.

2 High resolution images to be used for improving the analysis.

3 Also, use of other methods of measuring evaporation like the use Large Aperture Scintillometer (LAS) an instrument that measures the turbulent intensity of the refractive index fluctuations of air from the intensity fluctuations of a received signal for validation of the SEBS results. However, it is acknowledged that the costs acquiring and installing LAS is relatively high.

4 Use of SEBS at catchment and basin level to accurately estimate evaporation, this will lead to evaporation being incorporated in the hydrological models correctly and hence better management practices at catchment level.

REFERENCES

Allen, R.G. et al., 1996. Chapter 4: "Evaporation and transpiration, ASCE" *Handbook of hydrology*: 125-252

Anderson, J. R. et al., 1976. A Land Use and Land Cover Classification System for use with Remote Sensor data, Washington USA.

Anderson, M. C., Kustas, W. P., and Norman, J. M.: "Up scaling and downscaling – A regional view of the Soil-Plant Atmosphere continuum, Agron. J., 95, 1408–1423, 2003.

Avissar, R. and Pielke, R. A. 1989: "A parameterization of heterogeneous land surfaces for atmospheric numerical models and its impact on regional meteorology", Mon. Weather Rev., 117, 2113–2136,

Bastiaanssen W. G. M., Menenti M., Feddes R.A., Holtslag A.A.M. 1998a. "A remote sensing Surface Energy Balance Algorithm for Land (SEBAL)", Part 1: Formulation, *Journal of Hydrology* 212-213: 198-212.

Bastiaanssen W.G.M., Pelgrum H., Wang J., Ma Y., Moreno J., Roerink G.J., van der Wal T. 1998b. "The Surface Energy Balance Algorithm for Land (SEBAL), Part 2: Validation", *Journal of Hydrology* 212-213: 213-229

Beven, K., 1993. Prophesy, reality and uncertainty in distributed hydrological modelling. *Advances in Water Resources*, 16: 41-51.

Beven, K., 2004. Robert E. Horton and abrupt rises of groundwater. *Hydrological Processes*, 18(18): 3687-3696.

Bruijnzeel, L. A. 1990 "Forestation and dry flow in the tropics. A closer look, *Journal .Tropical .for Science*., 1 (3), 229-243.

Brutsaert, W., 2005 Hydrology: An introduction. Cambridge University

Calder, I. R., 1976 "The measurement of water losses from a forested area using natural lysimeter. *Journal of Hydrology* 30:311-325.

Calder, I. R., "Forests and hydrological services: Reconciling public and science perceptions" *Land Use and Water Resources Research* 2:2.1-2.12 http://www.luwr.com.

Cess R.D. 1978. "Biosphere-albedo feedback and climate modeling". *Journal of the Atmospheric Sciences*, 35:1765-1768

De Groen, M.M., 2002. "Modelling interception and transpiration at monthly time steps; introducing daily variability through Markov chains". PhD Thesis, IHE-Delft, Delft, the Netherlands.

Farah H.O., Bastiaanssen, W.M.G. 2001. Impact of spatial variation of land surface parameters on a regional evaporation: a case study with remote sensing data. *Hydrological Processes*.15(9):1585-1607.

Farah H.O., Bastiaanssen, W.G.M., Feddes, R.A. 2004. "Evaluation of the temporal variability of the evaporative fraction in a tropical watershed". *International Journal of Applied Earth Observation and Geoinformation* 5: 129-140.

Gallart, F. & Llorens, P., 2003. "Catchment management under environmental change: Impact of land covers change on water resources". *Water International*, 28(3) 334-340.

Hemakumara, H.M., Chandrapala, L., Moene, F.A., 2003. "Evapotranspiration fluxes over mixed vegetation areas measured from large aperture scintillometer". *Agricultural Water Management* 58, 109-122.

Jaspers, F.G.W., 2001. The new water legislation of Zimbabwe and South Africa: A comparison of legal and institutional reform. International Environmental Agreements: Policies, Laws and Economics 1:305-325.

Jaspers, F.G.W., 2003 "Institutional arrangements for Integrated Water River Basin Management". Water Policy 5:77-90.

Jackson, R. D.,W. P. Kustas, *et al.* (1988). "A re-examination of the crop water index." Irrigation Science **9**: pp.309-317.

Jia, L.,Z. Su, *et al.* (2003). "Estimation of sensible heat flux using the Surface Energy Balance System (SEBS) and ATSR measurements." *Physics and Chemistry of the Earth* 28(1-3): pp.75-88.

Kashaigili J. J., Kadigi, R. M. J., Sokile, C. S., Mahoo H. F., 2002. "Constraints and potential for efficient inter-sectoral water allocations in Tanzania. *WATERNET* meeting 2002 in Arusha.

Kimura, F. and Shimizu, Y., 1994. "Estimation of Sensible and Latent Heat Fluxes from soil surface Temp using a linear Air-Land Heat Transfer Model". *Journal of Applied Meteorology* 33(4): 477-489

Kongo V.M., Jewitt G.P.W. 2006. “Preliminary investigation of catchment hydrology in response to agricultural water use innovations: A case study of the Potshini catchment-S. Africa”. *Physics and Chemistry of the Earth*. 31:976–987.

Kustas, W. P. and J. M. Norman (1999). "Evaluation of soil and vegetation heat fluxes predictions using a simple two-source model with radiometric temperature for spatial canopy cover." *Agricultural and Forest Meteorology* 94: pp.13-29.

Kwast, J., Timmermans W., Gieseke, A., Su, Z., Olioso, A., L. Jia, J. Elbers, D. Karssenberg, S. de Jong. 2009. “Evaluation of the Surface Energy Balance System (SEBS) applied to ASTER imagery with flux-measurements at the SPARC 2004 site (Barrax, Spain)”, *Hydrology and Earth System Sciences*, 13, 1337–1347.

Jia, L., Z. Su, B. van den Hurk, M. Menenti, A. Moene, H.A.R. De Bruin, J.J.B.Yrisarry, M. Ibanez, A. Cuesta, 2003, Estimation of sensible heat flux using the Surface Energy Balance System (SEBS) and ATSR measurements, *Physics and Chemistry of the Earth*, 28(1-3), 75-88.

Li, Z.-L., L. Jia, Z. Su, Z. Wan, R.H. Zhang, 2003, A new approach for retrieving precipitable water from ATSR-2 split window channel data over land area, *International Journal of Remote Sensing*, 24(24), 5095–5117.

Liang, S., 2001, Narrowband to broadband conversions of land surface albedo I: Algorithms. Remote Sensing of Environment 76(2): pp.213-238.

Liang, S., J. S. Chad, et al., 2003, Narrowband to broadband conversions of land surface albedo: II. Validation. Remote Sensing of Environment 84(1): pp.25-41.

Lorup, K., Refsgaard, C., Mavzimavi, D., 1998. “Assessing the effect of land use change on catchment runoff by combined use of statistical tests and hydrological modeling: case studies from Zimbabwe”. *Journal of Hydrology*, 205 (1998) 147-163.

Maidment, D. R. 1993. *Handbook of hydrology*. Mc Graw-Hill, New York etc., 650pp

Meyer, W. B. and Turner II, B. L. 1992. “Human population Growth and global land use/cover change”. *Annual review of Ecological Systematic*; 2339-61.

Mohamed Y.A., Bastiaanssen W.G.M., Savenije H.H.G. 2004. “Spatial variability of evaporation and moisture storage in the swamps of the upper Nile studied by Remote Sensing techniques”. *Journal of Hydrology* 289 (2004) 145–164.

Monteith, J.L., 1965. “Evaporation and Environment: the state and movement of water in living organisms” *Symposium of .Social .Experiment* .Biology. 19:205-234.

Moran, M. S. 2004. Thermal infrared measurements as an indicator of plant ecosystem health, in: Thermal remote sensing in land surface processes, edited by: Quattrochi, D. A., and Luvall, J., Taylor and Francis, CRC Press, Boca Raton, USA, 257–282

Mu Q., Heinsch F.A., Zhao M., Running S.W. 2007. "Development of a global evapotranspiration algorithm based on MODIS and global meteorology data. Remote Sensing of Environment", doi:10.1016/j.rse.2007.04.015.

Nagler P.L., Glenn E.P., Kim H., Emmerich W., Scott R.L., Huxman T.E, Huete A.R. 2007. "Relationship between evapotranspiration and precipitation pulses in a semi-arid rangeland estimated by moisture flux towers and MODIS vegetation indices". *Journal of Arid Environments* 70:443-462.

Nnunduma A. B., 2005 "Water basins for consideration in order of priority". Ministry of Water and Livestock development of Tanzania, Dar es Salaam.

Pidwirny, M., 2006 Evaporation and Transpiration: Fundamentals of Physical Geography, 2nd Edition. http//www.pysicalgeography.net/fundamentals/8i.html.

Rahman, H. and G. Dedieu, 1994, SMAC : a simplified method for the atmospheric correction of satellite measurements in the solar spectrum . *International Journal of Remote Sensing*, 1994, vol.15, no.1, 123-143.

Schmugge T.J., Kustas W.P., Ritchie J.C., Jackson T.J., Rango A. 2002. Remote sensing in hydrology. *Advances in Water Research* 25:1367-1385.

Schulze R.E., Horan M.J.C., Gray R. 2005. "Sensitivity studies of hydrological responses in the Thukela Catchment to spatial and temporal representations when using a baseline and a projected future climate scenario. *In*: Schulze, R.E. (ed.). Climate Change and Water Resources in Southern Africa: Studies on Scenarios, Impacts, Vulnerabilities and Adaptation. Water Research Commission, Pretoria, RSA, WRC Report 1430/1/05. 211 – 232.

Sobrino, J.A. and N. Raissouni, 2000, Toward remote sensing methods for land cover dynamic monitoring: Application to Morocco, *International Journal of Remote Sensing* 21, pp. 353–366.

Sobrino, J.A. and N. Raissoini ,2003, Surface temperature and water vapour retrieval from MODIS data, International Journal of Remote Sensing VOL. 24, NO. 24, 5161-5182.

Su, Z., T. Schmugge, W.P. Kustas, W.J. Massman, 2001, An evaluation of two models for estimation of the roughness height for heat transfer between the land surface and the atmosphere, Journal of Applied Meteorology, 40(11), 1933-1951

Su, Z., 2002. “The Surface Energy Balance System (SEBS) for estimation of turbulent heat fluxes”. *Hydrology and Earth System Sciences*, 6(1):85-99.

Su, Z., A. Yacob, Y. He, H. Boogaard, J. Wen, B. Gao, G. Roerink, and K. van Diepen, 2003, Assessing Relative soil moisture with remote sensing data: theory and experimental validation, *Physics and Chemistry of the Earth*, 28(1-3), 89-101.

Su, Z., 2005, Estimation of the surface energy balance. In: Encyclopedia of hydrological sciences : 5 Volumes. / ed. by M.G. Anderson and J.J. McDonnell. Chichester etc., Wiley & Sons, 2005. 3145 p. ISBN: 0-471-49103-9. Vol. 2 pp. 731-752.

Tasumi M., Allen R.G., Bastiaanssen W. 2000. The theoretical basis of SEBAL, in ‘Application of the SEBAL Methodology for Estimating Consumptive Use of Water and Streamflow Depletion in the Bear River Basin of Idaho through Remote Sensing’. Idaho Department of Water Resources, University of Idaho, Department of Biological and Agricultural Engineering. Final report, pp. 46–69.

Timmermans, W. J.,J. van der Kwast, *et al.* (2005). “Intercomparison of energy flux models using ASTER imagery at the SPARC 2004 site (Barrax, Spain)”. ESA proceedings WPP-250 : SPARC final workshop, Enschede.

Tsiko, C.T., Makurira H., Gerrits A.M.J., Savenije H.H.G 2010. Measuring forest floor and Canopy Interception in a Savannah Ecosystem. *Physics* and Chemistry of the Earth (Submitted)

Valiente, J.A, Nunez, M., Lopez-Baeza, E. & Mereno, J.F. 1995. Narrow-band to broad-band conversion for Meteosat-visible channel and broad-band albedo using both AVHRR-1 and -2 channels, *International Journal of Remote Sensing* . 16(6): 1147-1166.

Wu W., Hall C.A.S., Scatena F.N., Quackenbush L.J. 2006. “Spatial modelling of evapotranspiration in the Luquillo experimental forest of Puerto Rico using remotely-sensed data”. *Journal of Hydrology* 328, 733–752.

Zhang, L., & Daves, W.R., Walker G.R., 2001. “Response of mean annual Evapotransipiration to vegetation changes at catchment scale.” *Water Resources Research* 37:701-708.

APPENDICES

The Wami Automatic Meteorological Station Data sets

30th June 2008

Wami-Prison 0001										
Date	Time	Precipitation	Temperature	Temperature Min.	Temperature Max.	rel. Humidity	Air Pressure	Wind Speed	Wind Direction	GRadiation
30.06.2008	01.00.00	0	16.9	16	17.3	91.7	973.7	0.3	281.2	0
30.06.2008	02.00.00	0	15.3	15	16	98.3	973.1	2.1	132.8	0
30.06.2008	03.00.00	0	15.4	14.9	16	98.8	972.7	1.2	172.9	0
30.06.2008	04.00.00	0	15.4	15.1	16	98.2	972.4	2.2	144.6	0
30.06.2008	05.00.00	0	14.6	14.2	15.1	99.9	972.6	1.1	54.8	0
30.06.2008	08.00.00	0	14.1	0	16.9	94.8	927.2	3.1	31.7	0
30.06.2008	09.00.00	0	19.8	17	21.3	81.4	975.6	4.6	19.1	0
30.06.2008	10.00.00	0	22.2	21	23.2	69	976.1	5.7	51.5	0
30.06.2008	11.00.00	0	24	23.3	24.5	64.4	975.7	6.2	79.9	1
30.06.2008	12.00.00	0	24.3	23.4	25.8	61.8	975.1	2.9	56.4	1
30.06.2008	13.00.00	0	26.1	25.2	26.8	53.4	974.1	3.8	166.5	1
30.06.2008	14.00.00	0	27	26.1	28.3	47.4	972.9	2.7	37.2	1
30.06.2008	15.00.00	0	27.6	26.7	28.5	45.2	971.9	1.5	331.8	0
30.06.2008	16.00.00	0	27.9	27.5	28.7	43.4	971	2.8	298.6	0
30.06.2008	17.00.00	0	28.2	27.3	29	42	970.6	2.8	327.8	0
30.06.2008	18.00.00	0	26.2	25.8	27.3	50.8	970.9	3.1	280.4	0
30.06.2008	19.00.00	0	24.7	23.8	25.8	58	971.4	1	242.6	0
30.06.2008	20.00.00	0	23.4	22.9	23.9	61.1	972	1.3	347.6	0
30.06.2008	21.00.00	0	21.6	19.9	22.9	72.7	972.5	1.6	99.6	0
30.06.2008	22.00.00	0	19.2	18.6	19.9	83.6	973.4	3.3	167.1	0
30.06.2008	23.00.00	0	18.7	17.8	19.1	82	973.8	1.8	142.7	0
30.06.2008	24.00.00	0	18.2	17.4	19.1	84.3	974.3	1.4	251.8	0

5th to 27th September 2008

Wami-Prison 0001											
Date	Time	Precipitation	Temperature	Temperature Min.	Temperature Max.	rel. Humidity	Air Pressure	Wind Speed	Wind Speed Max.	Wind Direction	GRadiation
25.09.2008	01.00.00	0	22.7	22.4	23	75.2	971.3	5.1	12.9	230.2	0
25.09.2008	02.00.00	0	22	21.6	22.4	78.3	970.7	2.8	8.7	243.3	0
25.09.2008	03.00.00	0	21.2	20.8	21.5	82.5	970.4	1.8	4.5	270.3	0
25.09.2008	04.00.00	0	20.2	19.8	20.8	89.3	970.4	0.8	3.6	348.9	0
25.09.2008	07.00.00	0	17.1	0	18.4	92.4	921.6	0.2	0.4	115.8	0
25.09.2008	08.00.00	0	20.3	18.5	22.2	90.3	973.3	0.5	6.4	144.6	0
25.09.2008	09.00.00	0	24.2	22.3	26.2	74	973.9	3.8	12.5	241.3	0
25.09.2008	10.00.00	0	26.5	25.7	27.4	62.1	974.2	5.5	16.2	245.3	1
25.09.2008	11.00.00	0	27.2	25.9	28.6	56.9	974.1	4.5	12.5	271.7	0
25.09.2008	12.00.00	0	28.8	27.7	29.8	48.6	973.2	4.3	17.5	245.9	0
25.09.2008	13.00.00	0	29.8	28.7	31	44.8	972	4.8	17.1	255.5	1
25.09.2008	14.00.00	0	31.2	30.4	32.2	38.7	970.8	5.8	16.2	276.3	1
25.09.2008	15.00.00	0	32.4	31.3	33.6	34.1	969.6	7.2	19.9	277	1
25.09.2008	16.00.00	0	31.8	31.4	32.8	33.8	968.9	6.3	22.4	267.1	0
25.09.2008	17.00.00	0	32	31.4	32.6	33.5	968.6	5.7	18.6	273.8	0
25.09.2008	18.00.00	0	31.6	30.8	32	33.9	968.7	3.2	15.2	279.3	0
25.09.2008	19.00.00	0	29.6	28.2	30.8	39.5	969.2	2	9.2	266.6	0
25.09.2008	20.00.00	0	27.8	27.3	28.1	50	970.1	4.4	15.2	245.1	0
25.09.2008	21.00.00	0	26.5	25.7	27.3	56.9	971	5.6	24.2	229.9	0
25.09.2008	22.00.00	0	25	24.5	25.7	61.1	972.1	8.7	23.2	244.7	0
25.09.2008	23.00.00	0	24.1	23.7	24.5	68.9	972.7	6.1	14.8	251.7	0
25.09.2008	24.00.00	0	23.3	22.7	23.7	77.4	972.8	6.3	19.9	250.1	0
26.09.2008	01.00.00	0	22.5	22.2	22.8	82.8	972.5	5.6	15.2	244.4	0
26.09.2008	02.00.00	0	21.9	21.7	22.2	85.9	971.9	5.9	15.2	256.5	0
26.09.2008	03.00.00	0	21.4	21.2	21.7	88.2	971.6	5	11.1	264.4	0
26.09.2008	04.00.00	0	21.2	21.1	21.4	90.1	971.5	5.1	13.3	252.5	0
26.09.2008	05.00.00	0	21	20.6	21.3	92.5	971.7	3.9	11.4	249.1	0
26.09.2008	07.00.00	0	17.4	0	19	91.9	898.7	0.2	0.4	126.8	0
26.09.2008	08.00.00	0	21.4	18.9	23.4	92.1	974.2	2.6	13.3	283.1	0
26.09.2008	09.00.00	0	24.4	22.6	25.7	73.1	975	4.9	14.3	276.5	0
26.09.2008	10.00.00	0	26.5	25	28.5	58.6	975.3	4	11.9	274.4	1
26.09.2008	11.00.00	0	28.4	27.5	29.3	46.2	975	4.4	25	299.7	1
26.09.2008	12.00.00	0	28.9	27.6	30.5	44.1	974	4	17.1	296.5	0
26.09.2008	13.00.00	0	30.1	28.9	31.1	38.8	972.8	4.9	17.1	268.6	1
26.09.2008	14.00.00	0	31.5	30.2	32.4	34.2	971.3	3.9	22.3	280	1
26.09.2008	15.00.00	0	32.1	31.3	32.9	31.5	969.9	3.7	16.7	253.8	1
26.09.2008	16.00.00	0	33.2	32.5	33.8	28	968.9	4.7	17.1	305.7	1
26.09.2008	17.00.00	0	33.2	32.7	33.5	27.4	968.4	4.5	13.1	273.6	0
26.09.2008	18.00.00	0	32.5	31.3	33.6	28.6	968.4	5.3	14.9	281.2	0
26.09.2008	19.00.00	0	30	28.6	31.3	34.4	968.9	4.6	15.7	293.2	0
26.09.2008	20.00.00	0	27.6	26.9	28.5	45	969.6	3.6	16.2	254.8	0
26.09.2008	21.00.00	0	26.1	25.5	26.8	60.6	970.9	7.6	17.5	231.3	0
26.09.2008	22.00.00	0	25	24.5	25.5	68.4	971.7	7.6	18.9	247.1	0
26.09.2008	23.00.00	0	24.2	24	24.5	77	972.3	6.1	13.7	244.6	0
26.09.2008	24.00.00	0	23.6	23.1	24	80.9	972.3	6.3	19.8	249.1	0
27.09.2008	01.00.00	0	22.7	22.4	23.1	83.7	971.8	5.7	15.6	248.7	0
27.09.2008	02.00.00	0	22.3	22.2	22.5	86.2	971.3	6.1	15.6	266.5	0
27.09.2008	03.00.00	0	22.7	22.5	22.8	84.7	970.9	4.9	13.3	258.4	0
27.09.2008	04.00.00	0	22.3	22.2	22.5	87.9	970.7	3.8	9.5	249.3	0
27.09.2008	07.00.00	0	20.4	0	22.1	83.9	902.6	3	5.4	281.6	0
27.09.2008	08.00.00	0	22.9	22.1	23.3	85.5	972.6	4.9	11.4	281.2	0
27.09.2008	09.00.00	0	25	23.3	26.1	72.5	973.2	6.1	16.2	266.8	0
27.09.2008	10.00.00	0	26.6	25.7	27.3	62.2	973.6	5.4	16.7	266.3	0
27.09.2008	11.00.00	0	28.7	26.7	30	50.5	973.4	5	17.7	248.4	0
27.09.2008	12.00.00	0	30.4	29.1	31.8	40.7	972.4	6	17.6	262.8	0
27.09.2008	13.00.00	0	30.6	29.7	32.3	39.2	971.1	4.9	16.2	275.1	1
27.09.2008	14.00.00	0	32	30.9	33.4	35.1	969.7	5.1	21.7	239.7	1
27.09.2008	15.00.00	0	32.8	31.9	33.6	32.7	968.4	7.4	17.6	250.5	1
27.09.2008	16.00.00	0	33.3	32.5	34	30.5	967.6	5.8	19	295	1

1st October 2008

01.10.2008	01.00.00	0	0	0	23.2	23.1	23.4	74.8	72.7	77	971.6	971.4	971.8	6.2	3.6	19.8	224.7
01.10.2008	02.00.00	0	0	0	23.4	23.2	23.5	72.1	71.2	73.1	971.2	970.9	971.4	5.8	2.6	14.3	24
01.10.2008	03.00.00	0	0	0	22.9	22.7	23.2	75.8	73.3	77.3	970.9	970.7	971	3.9	2.6	8.8	248.6
01.10.2008	04.00.00	0	0	0	22.1	21.5	22.7	81	77.4	84.4	970.5	970.3	970.7	3.2	0	7.3	264.2
01.10.2008	07.00.00	0	0	0	16.8	0	18.5	89	0	96.8	897.2	0	972	0	0	0.3	151.1
01.10.2008	08.00.00	0	0	0	21.6	18.6	23.9	84.6	74.1	96	972.4	972	972.8	1.8	0	8.3	133.1
01.10.2008	09.00.00	0	0	0	25.3	23.9	26.5	65.7	59	74.3	972.8	972.7	972.9	2.9	2.7	12	18
01.10.2008	10.00.00	0	0	0	27.3	26.2	28.4	55.2	48	61.3	972.7	972.5	972.8	2.4	2.8	14.4	197.8
01.10.2008	11.00.00	0	0	0	29	28	30.4	47	42.1	52.1	972.1	971.7	972.5	1.1	2.7	13.4	299.7
01.10.2008	12.00.00	0	0	0	30.2	29.7	31	39.7	36	43.9	971.2	970.6	971.8	4.6	2.7	16.7	276.4
01.10.2008	13.00.00	0	0	0	31.7	30.7	32.7	37.3	35.1	41.3	969.8	969.1	970.5	4.4	2.7	17.1	261.4
01.10.2008	14.00.00	0	0	0	32.9	31.7	33.7	34.6	32	37.9	968.3	967.6	969.1	2.8	3.7	16.8	246.5
01.10.2008	15.00.00	0	0	0	34.1	33.3	35.1	30.1	27.2	33	967	966.4	967.6	3.6	3.5	17.1	250.3
01.10.2008	16.00.00	0	0	0	35.2	34.6	35.8	26.9	25.8	28.4	966.2	966	966.5	4.5	0.4	14.9	296.3
01.10.2008	17.00.00	0	0	0	35.3	34.9	35.8	25.5	24.4	27.3	965.8	965.6	966	3.9	2.8	11.6	279.6
01.10.2008	18.00.00	0	0	0	34.4	33.1	35.5	27.6	24.8	30.4	965.9	965.6	966.1	6.3	2.8	16.8	284.5
01.10.2008	19.00.00	0	0	0	32	31.1	33.1	32.6	29.9	35	966.3	966	966.6	6.2	3.7	16.2	292.1
01.10.2008	20.00.00	0	0	0	29.7	28.2	31.2	44.5	34.8	54.3	967.1	966.6	968	8	2.7	22.3	265.4
01.10.2008	21.00.00	0	0	0	27	26.2	28.1	59.3	54.5	63	968.4	968	969	8.9	4.6	22.7	234.3
01.10.2008	22.00.00	0	0	0	25.6	25.1	26.1	63.5	62.3	65.1	969.4	968.9	969.8	9.4	5.5	27.8	234.4
01.10.2008	23.00.00	0	0	0	24.8	24.4	25.1	64.9	63.4	67.1	969.9	969.7	970.1	8.7	5.5	22.6	238.9
01.10.2008	24.00.00	0	0	0	23.9	23.5	24.3	71.1	67.1	74.8	970.2	970.1	970.3	7.1	4.5	18.9	238.2

28th July 2009

Wami-Prison 0001										
Date	Time	Precipitation	Temperature	Temperature Min.	Temperature Max.	rel. Humidity	Air Pressure	Wind Speed	Wind Direction	GRadiation
28.07.2009	01.00.00	0	17	16.3	17.9	79.9	975.8	1.3	204.7	0
28.07.2009	02.00.00	0	16.3	15.7	17	82.5	975.2	1.5	169.9	0
28.07.2009	03.00.00	0	16.9	16.4	17.4	81	974.6	0.8	259.9	0
28.07.2009	04.00.00	0	15.3	14.6	16.4	87.9	974.4	0.8	132.7	0
28.07.2009	05.00.00	0	15.3	14.7	15.7	88.2	974.5	0.8	178.3	0
28.07.2009	06.00.00	0	15.1	14.5	15.8	89.2	974.9	1.6	126.8	0
28.07.2009	08.00.00	0	14.6	0	16.8	89.8	975.7	1.9	70.3	55
28.07.2009	09.00.00	0	19.6	16.9	21.9	75.3	976.7	2.4	47.4	246
28.07.2009	10.00.00	0	23.1	21.9	24.5	58	976.7	3.3	64.4	434
28.07.2009	11.00.00	0	25.1	24	26	44.6	976.4	9.3	24.8	598
28.07.2009	12.00.00	0	26.6	25.9	27.2	38	976.1	7.4	356.6	700
28.07.2009	13.00.00	0	27.6	27	28.4	35.4	975.1	5.8	337.8	739
28.07.2009	14.00.00	0	28.6	27.6	29.4	33.1	973.8	3.1	27.3	718
28.07.2009	15.00.00	0	29.5	29.1	30.1	31	972.7	1.5	261.4	643
28.07.2009	16.00.00	0	30.1	29.4	30.6	30	971.8	2.1	252.8	512
28.07.2009	17.00.00	0	30	29.6	30.6	30.1	971.3	3.5	317.3	336
28.07.2009	18.00.00	0	29.8	29.3	30.3	32.4	971.6	0.8	238.4	112
28.07.2009	19.00.00	0	26.3	24.3	29.2	43.4	972	1.7	213.4	7
28.07.2009	20.00.00	0	23.6	22.7	24.3	48.4	972.3	1.5	301.8	0
28.07.2009	21.00.00	0	20.9	19.7	22.7	59.7	972.9	2.9	149	0
28.07.2009	22.00.00	0	19.6	19.1	20	66.5	973.1	2.8	122.9	0
28.07.2009	23.00.00	0	18.4	17.8	19	70.7	973.5	1.6	133.7	0
28.07.2009	24.00.00	0	18.8	17.8	19.7	68.4	973.8	3.4	238.9	0

25th September 2009

Wami-Prison 0001											
Date	Time	Precipitation	Temperature	Temperature Min.	Temperature Max.	rel. Humidity	Air Pressure	Wind Speed	wind speed Max	Wind Direction	GRadiation
25.09.2009	07.00.00	0	18.6	0	21.4	89.5	923.7	1.9	3.6	28	0
25.09.2009	08.00.00	0	22.1	19.6	23.9	85.7	972.9	4.2	12	261.4	0
25.09.2009	09.00.00	0	24.6	23.8	25.4	70.8	973.6	5.4	13	239.3	0
25.09.2009	10.00.00	0	26.5	25.1	27.6	59	973.8	4.6	12	264.7	1
25.09.2009	11.00.00	0	28.6	27.5	29.8	48.4	973.3	5.7	19.5	268.6	1
25.09.2009	12.00.00	0	29.3	28.1	31	45.4	972.4	6.1	19.5	278.9	0
25.09.2009	13.00.00	0	31.1	30.5	32.1	38.4	971.3	6.5	18.7	269.6	1
25.09.2009	14.00.00	0	32.2	31.2	33.3	33.5	970.3	9.2	24.6	280.8	1
25.09.2009	15.00.00	0	32.9	32.3	33.6	30.6	969.4	7.1	20.8	265	1
25.09.2009	16.00.00	0	33	32.2	33.8	30.4	968.8	8.7	24.3	265.2	1
25.09.2009	17.00.00	0	32.8	32.2	33.4	30	968.5	7	20.5	270.2	0
25.09.2009	18.00.00	0	32	31.3	32.9	31.8	968.6	6.3	18.7	269.4	0
25.09.2009	19.00.00	0	30.4	29.6	31.2	36.6	968.8	6	15.2	266.5	0
25.09.2009	20.00.00	0	28.7	27.9	29.6	47.2	969.3	7.6	18.5	250	0
25.09.2009	21.00.00	0	27.1	26.4	27.9	54	970.1	8.4	23.6	246	0
25.09.2009	22.00.00	0	25.8	25.5	26.3	54.5	970.7	9.1	25	242	0
25.09.2009	23.00.00	0	25	24.6	25.5	57.6	971.3	8.3	26.3	249.9	0
25.09.2009	24.00.00	0	24.2	23.8	24.6	69.5	971.4	9.3	17	257.1	0

If you use this worksheet, please acknowledge use as follows: Savage MJ, 2007. A spreadsheet for daily Penman-Monteith grass reference evaporation from a minimum set of meteorological data
Soil-Plant-Atmosphere Research Unit, School of Environmental Sciences, University of KwaZulu-Natal, Pietermaritzburg, South Africa

savage@ukzn.ac.za

Acknowledgements: CSI for images
Funding: WRC, UKZN

Sensors
Air temperature sensor for Tzmax and Tzmin

The CR200 datalogger (also contains a 2.4 GHz broad spectrum radio) allows grass reference evaporation to be calculated in real-time from hourly data. For further details, contact: cleroux@csafrica.co.za

Additional sensors
Solarimeter
Humidity sensor
Wind speed sensor
Wind direction sensor
Raingauge

References:
Savage, M.J. 1997. Introduction to Automatic Weather Station Systems for Measurement and Control. Zimbabwe Sugarcane Manual. Pp 28.

Station information	
Latitude (< 0 for southern hemisphere)	-6
Longitude	36
Altitude (m)	388
Grass reference reflection coefficient	0.23
Height zu of wind speed sensor (m)	2
Windiness of site: 0 for low, 1 for medium and 2 for high	1

Note: Use of this spreadsheet is at your own risk.

As far as possible, the equations used in this spreadsheet conform with those advocated by ASCE (2005): Task Committee on Standardization of Reference Evapotranspiration Environmental and Water Resources Institute of the American Society of Civil Engineers. January, 2005 Final Report

Is: solar irradiance (MJ m^{-2});
Tzmax: maximum air temperature (°C);
Tzmin: minimum air temperature (°C);
ez: water vapour pressure (kPa);
Uz: wind speed at 2 m (m s^{-1})

NOTE: If solar irradiance (column E) is not measured, leave it blank; it will then be estimated using the maximum and minimum air temperatures

Minimum set of data: Tzmax and Tzmin

Year	Day of year	Is	Tzmax	Tzmin	RHmaximum	RHminimum	U	Wind direction	Rainfall	Error comment	Grass reference evaporation
		(MJ m^{-2})	(°C)	(°C)	(%)	(%)	(m s^{-1})		(mm)		(mm)
2009	1									No error	
2009	2									No error	0.309
2009	3									No error	0.309
2009	4									No error	0.309
2009	5									No error	0.309
2009	6									No error	0.309
2009	7									No error	0.309
2009	8									No error	0.309
2009	9									No error	0.309
2009	10									No error	0.309
2009	11									No error	0.309
2009	12									No error	0.309
2009	13									No error	0.309
2009	14									No error	0.309
2009	15									No error	0.309
2009	16									No error	0.309
2009	17									No error	0.309
2009	18									No error	0.309
2009	19									No error	0.309
2009	20									No error	0.309
2009	21									No error	0.309
2009	22									No error	0.309
2009	23									No error	0.309
2009	24									No error	0.309
2009	25									No error	0.309
2009	26									No error	0.309
2009	27									No error	0.309
2009	28									No error	0.309
2009	29									No error	0.309
2009	30									No error	0.309
2009	31									No error	0.309
2009	32									No error	0.309

A spread sheet of Penman Monteith grass reference evaporation from minimum set of meteorological data.

During Ground Truthing visits- Wami at Dakawa Station

The Automatic Meteorology Station at Dakawa Prison Farm

The Mkindo River